

CONSIDERING HOLISTIC COASTAL RESPONSE TO CLIMATE-CHANGE INDUCED
SHIFTS IN NATURAL PROCESSES AND ANTHROPOGENIC MODIFICATIONS

Margaret Benham Jones

A thesis submitted to the faculty at the University of North Carolina at Chapel Hill
in partial fulfillment of the requirements for the degree of Masters of Science in the Department
of Geological Sciences.

Chapel Hill
2016

Approved by:

Laura J. Moore

A. Brad Murray

Tamlin M. Pavelsky

© 2016
Margaret B. Jones
ALL RIGHTS RESERVED

ABSTRACT

Margaret B. Jones: Considering holistic coastal response to
climate-change induced shifts in natural processes and anthropogenic modifications
(Under the direction of Laura J. Moore)

Shoreline erosion can prompt the implementation of local shoreline modifications (e.g., beach nourishment, seawalls) intended to prevent erosion and protect coastal investments. These localized modifications can cause additional, potentially adverse shoreline change in neighboring locations. Here, we explore coastline response to nourishment under different climate change scenarios by coupling two existing, complimentary models of coastal processes; one addressing shoreline change related to alongshore sediment transport and the other addressing cross-shore changes in barrier island position and geometry. Results of model experiments relevant to a case study on the Virginia coast, USA, highlight the importance of regional wave climate in determining how far-reaching the effects of nourishment activities will be and suggest that predictions of future changes in wave climate will be useful not only in determining where coordinated regional management strategies will be important, but also in forecasting required nourishment volumes.

ACKNOWLEDGEMENTS

Thanks to my advisor, Laura Moore, whose supportiveness and guidance kept this project on track. Many thanks also to Brad Murray, Dylan McNamara, Jonathan Whitley, and Michael Fenster for their helpfulness throughout this project. I'd also like to thank Andrew Ashton for assistance during model development and Gwynn Crichton and staff at The Nature Conservancy for instructive conversations. Tamlin Pavelsky provided helpful comments on a draft of this manuscript. This project was made possible through support provided by DOI and TNC, under the terms of Hurricane Sandy Coastal Resilience Fund grant # 42551 as administered by NFWF via sub-awards to the University of North Carolina at Chapel Hill, Duke University, University of North Carolina at Wilmington and Randolph-Macon College. The views and conclusions contained in this document are those of the authors and should not be interpreted as representing the opinions or policies of the U.S. Government or NFWF and its funding sources. Additional support was provided by the Martin Fund in the Department of Geological Sciences, University of North Carolina at Chapel Hill.

TABLE OF CONTENTS

LIST OF FIGURES	vii
LIST OF ABBREVIATIONS	viii
CHAPTER 1	1
1. Introduction	1
2. Background	3
3. Methods	6
3.1 Model Components	7
3.2 Model Initialization	9
3.3 Model Experiments	11
3.3.1 Sea Level Rise	11
3.3.2 Wave Climate	11
3.3.3 Nourishment	13
3.4 Change Analysis.....	13
4. Results.....	14
4.1 Effects of Climate Change Alone.....	14
4.2 Effects of Stabilization	16
5. Discussion	18

6. Conclusions.....	24
FIGURES	26
APPENDIX A: WAVE CLIMATE ANALYSIS	36
APPENDIX B: ALL RESULTS.....	37
REFERENCES	65

LIST OF FIGURES

Figure 1 – Study Site.....	26
Figure 2 – Schematic of Model Components	27
Figure 3 – Flow Diagram of Model Process	28
Figure 4 – Wave Climate Distributions	29
Figure 5 – Relative Sea Level Rise Results	30
Figure 6 – Wave Climate Change Results	31
Figure 7 – Comparison between Modeled Experiments and Added Results.....	32
Figure 8 – Nourishment Results for All Scenarios	33
Figure 9 – Limited Nourishment Spreading	34
Figure 10 – Amount of Required Nourishment	35

LIST OF ABBREVIATIONS

BIIMS	Barrier Island-Inlet Modeling System
BIM	Barrier Island Model
CEM	Coastline Evolution Model
E	East
IPCC	Intergovernmental Panel on Climate Change
NASA	National Aeronautics and Space Administration
NE	Northeast
NPS	National Park Service
RRSLR	Rate of Relative Sea Level Rise
RSLR	Relative Sea Level Rise
SCRD	Shoreline Change Rate Difference
TNC	The Nature Conservancy
USA	United States of America
USFWS	United States Fish and Wildlife Service
VA	Virginia
WFF	Wallops Flight Facility
WIS	Wave Information Systems

CHAPTER 1

1. Introduction

Barrier islands are dynamic, low-lying features occurring globally on gently sloping coastlines. In addition to their economic importance as vacation destinations and sites of commercial and residential development, barrier islands protect the mainland from storm impacts. However, as global climate continues to warm, barrier islands will be affected by climate-change induced increases in the rate of relative sea level rise (RRSLR; e.g. Mitchell et al., 2013; IPCC, 2014) and increases in the intensity of hurricanes or the frequency of the most intense hurricanes (e.g. Knutson et al., 2010; Emanuel, 2013). These effects will adversely impact development and the protective capacity of barrier island landforms (e.g., FitzGerald et al., 2008; Williams, 2013).

Barrier islands tend to respond to rising sea level by migrating upward and landward provided sufficient sand can be liberated from the shoreface and transferred to the top and back of the island via overwash, the movement of water and sediment across an island during storms or high water events (e.g., Bruun, 1962; Leatherman 1983; Cowell et al. 1995;). If barrier islands do not receive sufficient sand from the shoreface via overwash as sea level rises, they may not maintain sufficient elevation above sea level to remain subaerial and thus drown in place or disintegrate (e.g., FitzGerald et al., 2008; Moore et al., 2010; Lorenzo-Trueba and Ashton, 2014).

Increased RSLR rates in conjunction with coastal storms will lead to increased frequency and intensity of flooding in coastal areas (Woodruff et al., 2013). Importantly, increases in

hurricane intensity and increases in the frequency of the most intense hurricanes (Emanuel, 2013) will also alter wave climate along the U.S. East Coast. Such a shift in the recent past has been documented by Komar and Allan (2008), though not attributed to climate change. An increase in the frequency of intense hurricanes affects patterns of coastal erosion and accretion by altering the prevailing wave climate (specifically the angular distribution of wave influences), as shown by model simulations and observations of rates of coastal change (Slott et al., 2006; Moore et al., 2013; Johnson et al., 2014).

Stakeholders – organizations or individuals—who own or manage property along the coast often respond to coastal erosion by modifying the coastal zone in an attempt to “hold the line.” These efforts include beach nourishment (the addition of sand, typically from an offshore source) and shoreline armoring (the construction of physical structures such as seawalls or groins). As coastlines continue to change in response to changing climate, the tendency for humans to manipulate shoreline dynamics using these techniques will increase (Hapke et al., 2013; McNamara and Keeler, 2013). These manipulations in turn, alter both local and regional sediment budgets and nearshore processes, resulting in a strong two-way coupling between the human and natural components of the coastal system (Murray et al., 2013; Smith et al., 2015).

Although individual stakeholders and communities generally make management decisions independently of each other, previous work on multi-decadal to centurial rates of change on cusped coastlines demonstrates that the effects of stabilization can propagate alongshore, spreading non-locally due to wave shadowing, wherein a relatively seaward portion of the coastline reduces wave energy felt by other areas (Slott et al., 2010; Ells and Murray, 2012) altering patterns of shoreline change. Current decision-making processes rarely account for these spatially variable and extensive “neighbor” effects of stabilization efforts despite the

fact that this approach— wherein stakeholders make management decisions independently— could have negative economic consequences for neighboring stakeholders. In these cases, adverse effects may be mitigated by undertaking a more holistic, regional approach to coastal management (Lazarus et al., 2011; Williams et al., 2013).

Here, using a case-study approach, I seek to further understanding of the way in which RSLR and changes in storm activity will alter the coupling between the natural and human components of the coastal system on timescales relevant to human decision-making. Specifically, I seek to understand, for this case study: (1) How the patterns and rates of shoreline change vary with different RSLR and wave climate change scenarios, (2) How strongly stabilization efforts in one part of the system impact shoreline change rates in other parts of the system, and (3) How the effects of stabilization efforts on far-reaching parts of the coastline are altered by changes in RSLR rate and in wave climate.

In this work I focus on the Atlantic coastline of southern Maryland and Virginia, USA, and the stakeholders concerned with its management. Through discussions with local stakeholders I identified the climate change and coastal stabilization scenarios of greatest interest to managers of these barrier islands (Accomack-Northampton Planning District Commission, 2014). Through a series of 48 model experiments using a newly-developed model of coastline change, I evaluate the likely individual and future effects of a range of RSLR, wave climate change, and mitigation scenarios on future coastline evolution.

2. Background

The study area extends from the Maryland/Virginia border to the southern end of the Delmarva Peninsula on the Mid-Atlantic Coast of the United States. This region encompasses the Eastern Shore of Virginia and consists of an ~100 km stretch of 23 barrier islands and associated

inlets (Figure 1); the most prominent of the inlets is Chincoteague Inlet, located near the northern boundary of the study area between Assateague Island and Wallops Island. Prior work has identified this region as a hotspot of relative RSLR with modern relative RSLR rates of 3-4 mm/yr, which is 3-4 times the global average (Sallenger et al., 2012; Mitchell et al., 2013). Since the greatest proportion of wave influence in this region is from the northeast, the prevailing direction of alongshore sediment transport is from north to south. Although these islands are in close proximity to each other, they are owned by several different organizations, each with their own management goals.

Assateague Island, the northernmost of these barrier islands, is co-owned by the National Park Service (NPS, largely in Maryland) and the United States Fish and Wildlife Service (USFWS, in Virginia). The NPS manages Assateague Island with the goal of protecting and preserving its natural and cultural resources while allowing for public recreation on the island (National Park Service, 2002). The USFWS established the Chincoteague Wildlife Refuge in 1943 specifically to preserve habitat for migratory birds, and has since expanded their mission to include conservation of other resources as well as a commitment to providing public access for the over 1 million annual visitors who enjoy these resources (USFWS, 2015). To provide beach access in support of tourism, USFWS currently maintains a beach parking lot toward the southern end of Assateague Island; however, the expense of maintaining and repairing it after storm events is prompting the consideration of alternatives (USFWS, 2015). In this work, I explored the potential effects of beach nourishment designed to protect the parking lot. USFWS manages additional refuge acreage on nearby islands including Morris Island (located between Chincoteague and Assateague Islands), the northern end of Chincoteague Island, Assawoman Island, the northern end of Metompkin Island, and portions of Cedar Island.

The southern terminus of Assateague Island, now known as Fishing Point or Tom's Cove Spit, has prograded rapidly; the tip has been accreting southward at a rate of up to 55-65 m/yr since the mid-1800s (Leatherman et al., 1982; Schupp, 2013), sequestering sand delivered from the north. Fishing Point shadows nearby coastlines to the west and southwest from the effects of waves that approach from the northeast. Relatively little alongshore sediment transport occurs on the landward facing side of the spit, and the adjacent shorelines are protected from the prevailing northeasterly wave effects. Moving south along this partly sheltered shoreline, the exposure to those dominant northeasterly waves, and thus the southerly net alongshore sediment transport, increases. This gradient in net alongshore sediment transport creates an approximately 35 km "arc of erosion" south of Chincoteague Inlet (Galgano and Leatherman, 2005). As the end of Fishing Point spit extends progressively southward, the wave shadow zone also shifts southward, extending the arc of erosion. For the most part, islands within the arc of erosion have been eroding at rates of ~2-12.5 m/yr since at least the mid-1800s (Johnson et al., 2014).

Chincoteague Island, located west of southern Assateague Island, is home to ~3,000 residents of the Town of Chincoteague (U.S. Census Bureau, 2010). Due to its relatively sheltered location behind the most seaward island (Assateague Island), coastal change for Chincoteague is not addressed by this modeling work. Nevertheless, shifts in the patterns of erosion and accretion for other islands on the Virginia Eastern Shore also have the potential to affect Chincoteague because visits to the recreational beach on Assateague Island is a critical attraction for tourists who visit the Chincoteague community (USFWS, 2015).

Wallops Island, southwest of Assateague Island, is owned by NASA and houses the Wallops Flight Facility (NASA-WFF). The NASA-WFF management plan includes protecting more than one billion dollars of mission-associated assets located on the island (NASA, 2010).

As the northern-most barrier island in the “arc of erosion” Wallops has experienced historical rates of erosion in excess of 2.5 m/yr (Johnson et al., 2014). Following stabilization efforts, including the construction of a seawall in 1992, erosion rates have decreased to near 0 m/yr (Johnson et al., 2014; NASA, 2010).

The Nature Conservancy (TNC) manages an additional 14 mixed-energy barrier islands south of Wallops Island with the goal of allowing the islands and associated habitats to evolve naturally and to conserve land and water resources. The major islands (from north to south) include Metompkin, Cedar, Parramore, Revel, Hog, Cobb, Little Cobb, Ship Shoal, Myrtle and Smith. Because of their location in the arc of erosion, Metompkin, Cedar, and Parramore Islands have historically been highly erosional, having rates of retreat between -2 m/yr and -12.5 m/yr (Johnson et al., 2014; Leatherman et al., 1982).

3. Methods

To assess the effects that climate change and human modifications may have on patterns of erosion and accretion for this region, I coupled two existing models of coastal change (first described by Ashton and Murray, 2006a, 2006b and McNamara and Werner, 2008a, 2008b). The resulting Barrier Island-Inlet Modeling System (BIIMS, Figure 3) is an exploratory coastal change model that incorporates both alongshore and cross-shore processes. The modeling approach focuses on key interactions that are most directly responsible for decadal coastline change (alongshore sediment transport related to coastline orientation, wave forcing, wave shadowing, and barrier migration related to RSLR and inlet dynamics). With participation from stakeholders (Accomack-Northampton Planning District Commission, 2014), I developed inputs for a suite of model experiments that allowed me to systematically test the individual and cumulative effects of RSLR, wave climate change, and shoreline stabilization on multi-decadal

shoreline change rates. To represent the key dynamics of the region and assess the effects of these components, I developed a model coastline that shares important characteristics with the physical coastline, including general shape and qualitative patterns of shoreline change. Beginning with a simulated coastline formed from interactions and forcing the model allows me to isolate, by comparing a base case with each of the other 47 simulations, the patterns of changes associated with all combinations of climate and stabilization scenarios. Including the base case inputs, these scenarios include a total of 4 potential RSLR rate scenarios in combination with 3 possible wave climate distributions and 4 possible nourishment configurations (i.e. no nourishment, nourishment in the Assateague Island area only, nourishment in the Wallops Island area only, and nourishment at both sites).

3.1 Model Components

Because BIIMS is composed of two previously described and published models I provide only the most key elements here. For more details, I refer the reader to Ashton and Murray (2006a, 2006b) for a description of the Coastline Evolution Model (CEM), and McNamara and Werner (2008a, 2008b) for an in-depth presentation of the Barrier Island Model (BIM).

CEM is a one-contour-line model that simulates the plan-view evolution of a coastline based on alongshore gradients in alongshore sediment flux. Each model day CEM selects a new offshore wave approach angle from a probability density function (Figure 4), calculates wave shoaling and refraction (over implicit locally shore-parallel shoreface contours) until waves break in shallow depth, and then uses the CERC equation to calculate alongshore sediment flux. Coastline curvature tends to create gradients in alongshore sediment transport, and therefore changes in shoreline position. CEM also accounts for wave shadowing due to complex coastline shapes, which affects gradients in alongshore sediment transport (Figure 2a).

The primarily cross-shore model, BIM, idealizes a trapezoidal barrier island on an unerodible slope (Figure 2b). The model is forced by historical storm data collected by Zhang et al. who analyzed a record of U.S. Atlantic tide gauges spanning from the early 1900s to the end of the twentieth century and identified storm events (2000). During each model year, BIM draws a selection of storms based on these normal distributions of storm frequency, magnitude, and duration at the Hampton Roads, VA tide gauge. During model storm surge events, the water level rises and the island position adjusts in response. In the model, the upper shoreface erodes during storms, and eroded sediment moves to the sandbar reservoir, and to the top and back of the barrier. Between storms, the upper shoreface accretes. Inlets form in the model when the elevation of the top of the barrier falls below sea level as a result of erosion. Additionally, as sea level rises in BIM, the offshore toe of the shoreface moves up the continental slope, increasing the slope of the upper shore face of the barrier island and simulating barrier adjustment to RSLR (Stive and de Vriend, 1995).

Information passes between CEM and BIM each model year. At the beginning of each model year, CEM calculates alongshore sediment flux based on wave approach angles. BIIMS sums the net yearly sediment flux between each set of adjacent CEM cells, calculates the gradient in flux for each cell, and passes that information to BIM. This yearly process replaces the daily shoreline adjustments that CEM makes when running individually. In the coupled BIIMS, BIM adjusts cross-shore position of the barrier island in response to alongshore sediment transport gradients from CEM in addition to storm dynamics and RSLR. After BIM calculates the new shoreface position, BIIMS passes that information to CEM and the model iterates yearly from there.

3.2 Model Initialization

Prior to running BIIMS, I first initialize both components of the coupled model (i.e. CEM and BIM) separately. To initialize CEM, I begin from a plan view shoreline with 500 m resolution cells forming a blocky “arc” having approximately the same dimensions as the observed arc of erosion on the Virginia shore. To represent the approximate location and behavior of Chincoteague Inlet, on the north side of the block, I designate a line of cells, trending in the regional alongshore direction, as sediment sinks. Because of its status as a federal navigation channel, Chincoteague Inlet is usually dredged twice per year leading to the disposal of 7,000 m³ of sediment outside of the channel area (Hardaway et al., 2015). In addition, sediment is likely lost from the nearshore system to natural deposition in tidal channels landward of the inlet. Given a lack of quantitative constraints on how rapidly the inlet draws sand away from the adjacent shoreline, in the model I use a simple approach: half of the sediment that enters the sink representing this inlet is lost from the system.

In CEM I impose an erosion rate of 3 m/yr near the north end of the domain. This erosion rate was selected because (a) it produces a spit having approximately the shape and behavior of that observed at Fishing Point (Ashton et al., 2016) and (b) it is consistent with average recent rates of erosion of the northern end of Assateague Island (Johnson et al., 2014). Because I expect the alongshore-transport-maximizing coastline orientation (Ashton et al., 2001) to be achieved as waves approach the southern end of the Delmarva peninsula, I assign a boundary flux in the southern most cell (right-most portion of the domain) that has the same value as the maximum flux from the remainder of the domain as calculated at each timestep. This condition represents sediment lost into the Chesapeake Inlet or transported farther alongshore.

As this initial blocky configuration evolves with a WIS-derived wave climate (see section 3.3.2) for 200 model years, it achieves a shape and behavior approximately consistent with large-scale observations of plan-view shoreline change along the Delmarva Peninsula. Specifically, (a) the northern block produces a spit, which, like Fishing Point, arcs slightly west and progrades south at ~10-15 meters per year (as estimated from recent satellite data spanning 1984-2012), (b) the coast immediately downdrift of this spit erodes landward at approximately 2-3 m/yr (consistent with recent observations of the Wallops Island area coastline (Johnson et al., 2014)), and (c) the southern block “relaxes” into a plan-view curvature reminiscent of the portion of the Virginia Barrier Islands spanning from Cedar Island to Parramore Island.

To initialize BIM I begin from a barrier height of 1.7 m and width of 700 m, and a tidal prism of $27 \times 10^6 \text{ m}^3/\text{m}$ (representing the typical cross-shore width of the back-barrier basin multiplied by the elevation difference between high tide and the back-barrier sediment surface or between high tide and low tide, whichever is smaller) and spin up the model for 500 model years to achieve an equilibrium state (see McNamara and Werner 2008a for further detail on parameters and values). To smooth stochastic effects from model spin up, I use the alongshore average of important geometric characteristics such as island height, width, and position at the end of the spin up period as the starting point for the BIM component of the coupled model system (BIIMS). In a separate suite of runs analyzing the potential for inlet opening, I initialize BIM with a barrier height of 1.1 m and width of 700 m and adjust the tidal prism to $5.6 \times 10^6 \text{ m}^3/\text{m}$. For model runs investigating inlets, I initialize the model with 3 inlets (outside the domain of interest) so that the BIM domain is starting from an inlet density and tidal prism relationship that is more consistent with the configuration observed in this region (this alters inlet opening but does not appreciably change shoreline change rates).

3.3 Model Experiments

To compare shifts in coastline change patterns arising from different climate and nourishment scenarios, I first developed a base case model run which did not include nourishment. The base case RSLR rate, held constant in time, is an extrapolation of the currently observed linear rate of 3 mm/yr (Sallenger et al., 2012; Mitchell et al., 2013). The wave climate is the same WIS-derived wave climate (see section 3.3.2) used during model initialization.

3.3.1 Sea Level Rise

The three “Low,” “High,” and “Highest” experimental sea level rise cases are non-linear scenarios created based on global data and adjusted for the study area (Mitchell et al., 2013). (An additional “Mid” sea level rise scenario exists for this region; however discussions with stakeholders revealed the other three to be of greater interest to local managers). The “low” scenario is based on conservative assumptions about future greenhouse gas emissions, the B1 scenario, and accounts for RSLR due primarily to ocean warming (Parris et al., 2012). The “high” scenario accounts for some limited ice sheet loss and is based on the upper end of projections from semi-empirical models. The “highest” scenario is a current practical worst-case scenario that includes maximum contributions from ice sheet loss and glacial melting (Pfeffer et al., 2008). The “low,” “high,” and “highest” scenarios include 1.1, 1.7, and 2.5 meters of total RSLR over the 50-year model run, respectively.

3.3.2 Wave Climate

Previous work has shown that plan view coastline shape and evolution depend on the angles at which waves approach the coast. Although the approach angle and height of waves changes on a time scale of hours to days, multi-kilometer-scale patterns of shoreline change typically arise from gradients in net sediment flux that accrue over substantial time—decades to

centuries or longer (Lazarus et al., 2011). Taken in aggregate, this wave climate includes the effects of storms and seasonal patterns (Ashton and Murray, 2006a, 2006b).

Following the approach of Johnson et al (2014) I developed the wave climate distributions used in this study using Wave Information Systems (WIS) hindcast data from virtual buoy 63177, located 27 km SE of the southern end of Assateague Island in a water depth of 25 m for 1980 - 2012 (data available from <http://wis.usace.army.mil/>). WIS datasets provide a variety of wave characteristics, including wave height and angle of approach, at hour-long intervals spanning 1980-2012. I divide these data into 15° bins by wave approach angle relative to the general coastline trend (Figure 4a). The distribution centers around -30° (waves approaching from 30° counterclockwise from a shore-normal direction for the average coastline orientation—i.e. a majority of wave influence is from the E to NE) (Figure 4b), which is consistent with observed net transport from north to south.

Given the documented effect of increasing hurricane strength on wave climate (Moore et al., 2013; Johnson et al., 2014), I address changes in storm intensity in the model by adjusting the WIS-derived wave climate used for model initialization and the base case run to reflect either a higher angle wave climate representing a greater proportion of waves approaching from the northeast (increased influence of storm-derived waves; Moore et al., 2013) or, for comparison, a lower angle wave climate representing a lesser proportion of waves approaching from the northeast (decreased influence of storm-derived waves). I accomplished this by modifying the original WIS data to create two hypothetical wave climate distributions. To create the higher angle wave climate distribution, I rotated the angle of approach for all waves in the distribution by negative 15°, representing a greater proportion of waves approaching from the NE (Figure

4b). The “lower angle” wave climate distribution rotates the angle of approach for all waves by positive 15° , representing a lesser proportion of waves approaching from the NE (Figure 4c).

3.3.3 Nourishment

Based on stakeholder input (Accomack-Northampton Planning District Commission, 2014) I identified two zones within the study area (corresponding roughly to sties on Assateague Island and Wallops Island) where nourishment activities are likely to take place in the future. I modeled the Assateague nourishment zone as a 2 km (4 cell) stretch and the Wallops nourishment zone as a 4 km (8 cell) stretch. At each yearly timestep, BIIMS calculates the volume of sand lost during the previous year and adds that volume, assumed to be derived from outside the model domain, back to the shore face to maintain the initial shoreline position for the duration of the run.

3.4 Change Analysis

To determine shifts in patterns of coastline change associated with each climate change scenario, I calculate the shoreline change rate difference (SCRD). The SCRD is the difference in shoreline change rates between the 50-year base case scenario and the experimental scenario in question, at each alongshore location. A negative SCRD indicates that the experimental scenario results in more erosion or less accretion relative to the base case, whereas a positive SCRD indicates that the scenario results in more accretion or less erosion relative to the base case. To discern the effects of nourishment on coastline change, I also compare each scenario that includes nourishment to its corresponding climate change scenario without nourishment (Figure 8). The effects of nourishment are relatively small, so presenting the SCRD relative to the base case for nourishment scenarios obscures the subtle differences resulting from nourishment in favor of the more obvious climate change signals. In addition to calculating the SCRD for each

scenario, I measure island height as a function of alongshore distance at the end of each 50-year simulation experiment as a means for assessing alongshore variations in the potential for inlet opening.

4. Results

4.1 Effects of climate change alone

To determine the effects of RSLR in absence of nourishment or wave climate change, I held the wave climate constant without nourishment and ran the model for each RSLR scenario. For each relative sea level rise scenario (low, high, and highest) the effects of RSLR are variable alongshore: some areas are more responsive whereas others are less responsive. For all RSLR experiments, the portion of the domain representing the southern end of Assateague Island has a larger negative SCRD relative to the rest of the domain. This effect is strongest for the highest RSLR scenario (when the SCRD in the portion of the domain representing the southern end of Fishing Point is 5 m/yr more negative than the domain average). During the low RSLR scenario, the SCRD in the portion of the domain representing the southern end of Fishing Point is 3 m/yr more negative than the domain average (Figure 5). In contrast, although the portion of the domain representing Wallops Island erodes more quickly in the RSLR scenarios relative to scenarios without RSLR, it is affected less strongly by RSLR than the rest of the domain. In all three RSLR scenarios, for the portion of the domain representing Wallops Island, the SCRD is 1-2 m/yr less negative than the domain average, meaning that relatively less erosion or more accretion occurs in this area (Figure 5).

Wave climate shifts also affect patterns of erosion and accretion and in ways that vary alongshore. When a greater proportion of wave influence is from the NE (higher angle), a 7-km stretch along the portion of the domain representing the southern end of Assateague Island

experiences approximately 2 m/yr more accretion or less erosion whereas a 14-cell portion of the domain representing the Wallops Island area experiences approximately 1 m/yr more erosion (Figure 6a). When the wave climate distribution is such that a lesser proportion of wave influence is from the NE (lower angle), an 11-km portion of the domain representing Wallops Island experiences up to 2 m/yr more accretion or less erosion, and an 8-km portion of the domain representing the southern end of Assateague Island experiences up to 4 m/yr more erosion or less accretion (Figure 6b).

As in the scenarios for wave climate change alone, when RSLR and wave climate change are both included, a higher wave angle distribution and lower wave angle distribution leads to less negative SCRDs for the portions of the domain representing Assateague Island and Wallops Island, respectively. Although the patterns of shoreline change in these combined runs broadly correspond to the independent effects of each scenario, the effects of RSLR and wave climate change modeled independently are not strictly additive. For the scenario in which a greater proportion of waves approaches from the NE (higher angle), the simple addition of SCRDs from the independent RSLR and wave climate change scenarios tends to under-predict the SCRD for the portion of the domain representing Assateague Island (by up to 2.5 m/yr) (Figure 7). Similarly, in the case where a lesser proportion of waves approach from the NE (lower angle), the simple addition of shoreline change rates under-predicts the SCRD for the portion of the domain representing Wallops Island by a similar margin. The non-linear response of coastline change to sea level rise which is captured in the model explains this important difference (and is elaborated on in the Discussion section).

In some runs, I observe an enhanced potential for inlet opening relative to the recent past for specific alongshore locations. When a greater proportion of wave influence is from the NE

and the RSLR scenario is “high” or “highest,” there is a greater potential for inlet opening in the portion of the domain representing Wallops Island (approximate alongshore cell number 137). When a lesser proportion of wave influence is from the NE and the RSLR scenario is “high” or “highest,” there is a greater potential for inlet opening in the portion of the domain representing Assateague Island (approximate alongshore cell numbers 101-104). Neither RSLR nor wave climate change independently are associated with enhanced inlet opening in either of these areas, suggesting that the higher rate of erosion caused by the combination of climate change factors may be necessary to enhance the potential for inlet opening.

4.2 Effects of stabilization

I conducted simulations in which Assateague Island and Wallops Island are nourished individually as well as scenarios in which they are nourished concurrently. However, because none of the scenarios showed appreciable effects on shoreline change rate outside the immediate vicinity of each individual nourishment zone (indicating that the effects of nourishment at each site can be evaluated individually even in experiments in which both sites are being nourished), we present only the results of simulations in which both sites were nourished simultaneously.

To discern the effects of nourishment in model runs, we compare each scenario that includes nourishment to its corresponding climate change scenario without nourishment (Figure 8). If nourishment has an effect on shoreline change outside of the nourished zones, we would expect to see altered shoreline positions immediately adjacent to the nourishment site that merge continuously into the nourished areas and into rest of the shoreline farther from the site (as in Slott et al, 2006; Ells and Murray, 2012). With limited exceptions, discussed below, such signals of alongshore-extended nourishment effects are not evident in Figure 8. In contrast, most prominent are the undulations appearing between the two nourishment zones in the curves

showing the differences between model runs. These undulations arise from stochastic undulations in shoreline position that occur in all scenarios (including non-nourishment scenarios) due to model discretization, as discussed in detail in the Discussion section. When calculating the difference between runs involving nourishment and the equivalent scenario without nourishment, these stochastic differences in the shoreline-position undulations appear in the shoreline position difference signal and do not represent signals of alongshore-extended nourishment effects.

I conclude, then, that in the absence of RSLR, beach nourishment seems to have almost no effect outside of the nourishment zones regardless of which of the three wave climate scenarios are used (blue lines on Figure 8 a-c). Nourishment also has no effect on the potential for inlet opening described in the previous section. For cases of low, high, or highest RSLR with no wave climate change (Figure 8a), or with a lower angle wave climate (Figure 8b), any possible nourishment signal from the Assateague Island nourishment zone (possibly represented by altered shoreline position differences immediately to the north and south) appears limited in alongshore extent (within 2 km). In these scenarios, in the portion of the domain south of the 4-km Wallops Island nourishment zone a potential consistent alongshore effect of nourishment may be discernible up to 5 km (10 cells) from the nourishment zone. In the case of the higher angle wave climate change scenarios (Figure 8c), shoreline change patterns north of the Assateague Island nourishment zone and south of the Wallops Island nourishment zone there appears to be a 2 km additional nourishment signal on the north side of the Wallops Island nourishment zone.

General patterns of accretion and erosion observed for different climate change scenarios are relevant to nourishment decisions because they affect the total nourishment volume that will

be required to maintain shoreline position. The biggest determinant of erosion rates and therefore the nourishment volumes necessary to maintain initial shoreline position is the sea level rise rate (Figure 10). In the base case RSLR, the average volume of sand needed is $\sim 150 \text{ m}^3/\text{m}$. The average volume of sand needed for the highest RSLR case is two orders of magnitude greater at $\sim 10,000 \text{ m}^3/\text{m}$. Wave climate also has a secondary effect on the erosion rates and therefore the total volume of nourishment needed. For example, for wave climates having a greater proportion of influence from the NE, the Wallops Island area needs an average of $\sim 400 \text{ m}^3/\text{m}$ more nourishment compared to Assateague Island over the course of 50 years to achieve the same steady shoreline position (a 10% difference). Given a current estimated cost of beach nourishment of $\$15/\text{m}^3$ (USFWS, 2015), this translates to an average difference in cost for the volume of sand needed over 50 years between these two sites of $\sim \$6,000/\text{m}$. Note that even for cases in which a lower proportion of wave influence is from the NE (favoring lower nourishment volumes per alongshore meter in the Wallops Island portion of the domain), the Wallops Island site still requires twice the total volume of nourishment needed for the Assateague Island site because the nourished length of shoreline is twice as long (Figure 10b).

5. Discussion

This modeling approach focuses on the interactions that are most directly responsible for decadal coastline change. These include alongshore sediment transport related to coastline orientation, wave forcing, the effect of wave shadowing, and barrier migration related to RSLR and inlet dynamics. The resulting model domain shares important characteristics with the actual coastline, although it does not correspond in detail. The goal is to use this model to assess how patterns of coastline change may tend to shift under a range of different climate change scenarios—my assessments are meant to be qualitative in both the temporal and spatial sense.

Future work with coupled cross-shore and alongshore models could build on these results by refining the representation and analysis of inlets and other barrier island processes and revising wave climate change scenarios based on current projections (for example Storlazzi et al., 2015).

I observe that the net result of adding shoreline change rates from a RSLR experiment with those from a wave climate change experiment is different from the result obtained by running a combined RSLR and wave climate change experiment (Figure 7). Specifically, the combined experiment results in higher rates of erosion than the additive case in areas of the domain whereas the wave climate change scenario alone results in more accretion relative to the base case. As sea level rises in BIIMS, the amount of shoreline retreat due to RSLR is a non-linear function of the cross-shore position, with positions farther offshore experiencing greater rates of change because the shoreface is steeper in those areas. For areas of the domain in which wave climate change results in more accretion or less erosion relative to the base case (a positive SCRD), rates of change due to RSLR are higher than they would be otherwise. This effect also explains the alongshore differences in coastline response to RSLR arising from my experiments: the Wallops Island area is more erosional than the rest of the domain, therefore it responds less strongly to RSLR relative to the rest of the domain. I also find that a high or highest RSLR rate in conjunction with higher angle wave climate leads to an increased tendency for inlets to open in the Wallops zone; however current management actions at Wallops Island (including a rock seawall and nourishment plan) are unlikely to permit inlet formation.

In all model scenarios, I observe relatively high-amplitude undulations in the portion of the domain roughly corresponding to the southern end of Assateague Island and the northern part of Wallops Island (roughly from cells 50 to 150). These undulations arise from a combination of factors having to do with the modeling process. The relatively high curvature in that area in

conjunction with the regional wave climate produces small undulations with stochastic positions. When the CEM model timestep is one day, these perturbations tend to be smoothed; however the yearly model timestep used in BIIMS amplifies these perturbations. This observation motivates future work on decreasing the timescale of the coupling (from yearly to daily).

In the model, I assume that beach nourishment continues over 50 years at rates sufficient to maintain a fixed shoreline position without regard for the cost of nourishment. However, my results show that the estimated total volume of sand required for nourishment will vary widely depending on the climate change scenario (depending mostly on RSLR rate, with a secondary effect from wave climate change). Given a current estimated cost of beach nourishment of \$15 per m^3 (USFWS, 2015), model-derived estimates for the total volume and cost of nourishment across all simulations range from 1.8 m^3/m or \$28,000/m for the low RSLR scenario to 10 m^3/m or \$150,000/m for the highest RSLR scenario. This represents a total estimated cost of nourishing both sites (6 km total) of ~\$170 million to \$920,000 million over 50 years. I expect fulfilling a commitment to shoreline stabilization will become more expensive in the future (due to increased volumes of sand required for nourishment as well as likely changes in the price of sand as demand increases), and thus nourishment plans are likely to be reassessed in the future. Additionally, previous work using coupled economic-physical models has shown that the dynamics of beach nourishment depend on regional interactions between patterns of property value and erosion as well as property owner attitude regarding climate risk (McNamara et al., 2011; McNamara and Keeler, 2013) and that when multiple property owners make nourishment decisions independently, emergent behaviors in patterns of shoreline erosion and accretion can also affect future nourishment decisions (Lazarus et al., 2011).

Surprisingly, I found that the alongshore effects of beach nourishment are likely to be limited in this region. Although I observe an alongshore signal of nourishment extending up to 5 km away from the Wallops Island nourishment zone, I see a comparatively alongshore-limited signal at the Assateague Island nourishment site. Here, nourishment effects appear to be limited within 1 km of the nourishment zone. This is in contrast to previous work that found the effects of beach nourishment to be non-local with signals of change extending tens of kilometers or more from zones of nourishment (Slott et al., 2010; Ells and Murray, 2012). To understand this difference, I need to consider how relative wave approach angles influence patterns of erosion and accretion.

When waves approach from less than $\sim 45^\circ$ relative to local coastline orientations (i.e., ‘low angle’ waves; Ashton and Murray 2006b), gradients in alongshore sediment transport tend to smooth out, or diffuse, coastline undulations (e.g. Ashton and Murray, 2006a, b). Alternatively, when waves approach the coast from relative angles greater than $\sim 45^\circ$ (i.e., ‘high-angle’ waves) waves exert an ‘anti-diffusive’ influence on coastline shape, tending to make plan view undulations grow (i.e. roughing of coastline undulations rather than smoothing). Along any coast, waves will sometimes approach from low angles (relative to the coastline orientation), and sometimes approach from high angles. Whether coastline undulations diffuse or grow over time depends on the mix of these low- and high-angle wave influences (Ashton and Murray, 2006b).

Local wave climates are typically dominated by low-angle wave influences (Ashton and Murray, 2006b), and previous studies addressing the alongshore effects of nourishment have involved such locally diffusive wave climates (Ashton and Murray 2006b). Ongoing local nourishment on an eroding coastline leads, over time, to a subtle coastline protuberance where the shoreline is stabilized. Under typical, diffusive local wave climates, alongshore sediment

transport gradients tend to smooth this subtle coastline bump, which causes the effects of the nourishment to spread alongshore (Slott et al., 2010; Ells and Murray, 2012).

In contrast, within this study area, local wave climates are atypical. The distributions of wave influence relative to the general coastline trend (Figure 4) are such that most of the wave influence is from relative approach angles close to 45° . Waves approaching from approximately 45° do not produce either a smoothing or roughening effect on coastline shape (e.g. Ashton and Murray, 2006a, b). In addition, given the unimodal wave climate centered on $\sim 45^\circ$ relative to the coastline orientation, the influence on alongshore sediment transport from high-angle and low-angle waves is approximately equal (Figure 4). Therefore, net wave influence along most of the coastline is approximately balanced between diffusive and anti-diffusive wave influences (i.e., the coast has near zero net diffusivity). The finding that the nourishment signal does not spread alongshore is consistent with the balance between diffusive and anti-diffusive wave approach angles specific to this study area. Model experiments using CEM alone (Figure 9), show that nourishment tends to have more limited alongshore effects when the wave climate is closer to no net diffusivity. It is important to note that although shoreline stabilization through beach nourishment does not affect adjacent parts of the coastline in this study, stabilization through the use of hard structures would have an affect on downdrift portions of the coastline, regardless of the net diffusivity of the local wave climate.

The stochastic undulations in shoreline position, and therefore in shoreline-position differences (Figure 8), complicate the evaluation of nourishment effects outside the nourished areas. In all model scenarios, these undulations occur in the portion of the domain roughly corresponding to the southern end of Assateague Island and the northern part of Wallops Island (roughly from cells 50 to 150). These undulations arise from a combination of factors. The net

diffusivity of the wave climate is especially close to 0 for this portion of the domain, where the mean of the wave-climate distribution falls even closer to $\sim 45^\circ$ relative to local coastline orientations mean than it does for the regional average coastline orientation. In addition, using annual time steps instead of daily time steps in CEM, in combination with the ~ 0 net diffusivity in this region, gives rise to model artifacts. When the CEM model time step is one day, subtle shoreline-shape perturbations with relatively small alongshore length scales tend to be smoothed out by the low-angle waves in the wave climate. Such smoothing occurs even if the low-angle wave influence is approximately balanced by high-angle wave influences. However, with the yearly model timestep used in BIIMS, only annual net sediment fluxes are passed from CEM to BIM, and the smoothing effects of the low-angle can be lost when the net diffusivity is ~ 0 . Thus, undulations in this portion of the domain can grow. This observation motivates future work on decreasing the timescale of the coupling (from yearly to daily).

However, despite the complications in detecting alongshore-extended nourishment effect in Figure 8 that these undulations cause, we are confident in the conclusion that the alongshore extend of nourishment effects is very limited in this case-study region. Figure 10, which does not involve the complicating undulations, shows that nourishment effects tend to become more spatially localized as the net diffusivity of the wave climate decreases.

Further, my findings suggest that regional wave climate and, perhaps more importantly, anticipated future regional wave climate, may dictate whether or not a holistic, regional approach to coastal management involving beach nourishment will be necessary to insure the maximum good for the greatest number of coastal stakeholders. Where the wave climate and coastline orientation combine to produce diffusive, coastline-smoothing wave influences, localized shoreline stabilization has significant spill-over effects to neighboring parts of the coastline,

raising the possibility that a coordinated management strategy could be more effective than a strictly local management strategy. In such a case, the net benefits to the nourishing communities combined with those of the adjacent communities can be jointly maximized. However, where the effective diffusivity (integrated over the wave climate; Ashton and Murray 2006b) is close to 0 (the less likely of the two situations), nourishment decisions in individual communities are not coupled through the coastline smoothing mechanism, so that holistic management (in the case of nourishment only) will not likely provide additional benefits. These results suggest that assessments of current and future regional wave climate may be important in identifying coastal areas that will benefit from a holistic approach to coastal management as climate change brings about shifts in environmental conditions that affect patterns and rates of shoreline change.

6. Conclusions

By coupling two numerical models of coastline change and exploring a range of climate scenarios (three accelerated RSLR scenarios and two wave climate change scenarios) and shoreline stabilization scenarios (two independently-controlled nourishment zones), I have developed a suite of results illustrating how multi-decadal patterns of coastline erosion and accretion could change for a region along the Mid-Atlantic Coast of the U.S. under different combinations of future conditions.

In the absence of nourishment, the entire coast is likely to erode more quickly (or accrete more slowly) at higher RSLR rates relative to a scenario with only a modest, linear rate (3 mm/yr) of RSLR. The effects of RSLR vary alongshore, such that the southern end of Assateague Island is more affected by RSLR and the Wallops Island area is less affected by RSLR relative to the rest of the domain. Changes in wave climate affect localized portions of the domain on either side of the Assateague Island spit: a greater (lesser) proportion of waves

approaching from the NE increases erosion by 2-4 m/yr in the portion of the domain representing Wallops Island (Assateague Island) relative to the base case.

As RSLR increases, the volume of nourishment sand required to maintain the position of the shoreline increases as well (as expected). Shifts in wave climate patterns also increase or decrease the required nourishment volume in specific zones. In contrast to previous studies, in the absence of increased RSLR, nourishment has essentially no effect on coastline change rates outside of the nourished zone because the wave climate in this region has close to zero net diffusivity, which is likely to be a relatively unusual case. These results have implications for coastal management, suggesting that in this specific location and other regions having a similar wave climate, a regional, holistic approach to beach nourishment will not likely provide additional benefits. This work highlights the importance of wave climate in determining where holistic nourishment strategies may be most beneficial and in assessing future patterns of shoreline change as well as in forecasting required nourishment volumes.

FIGURES

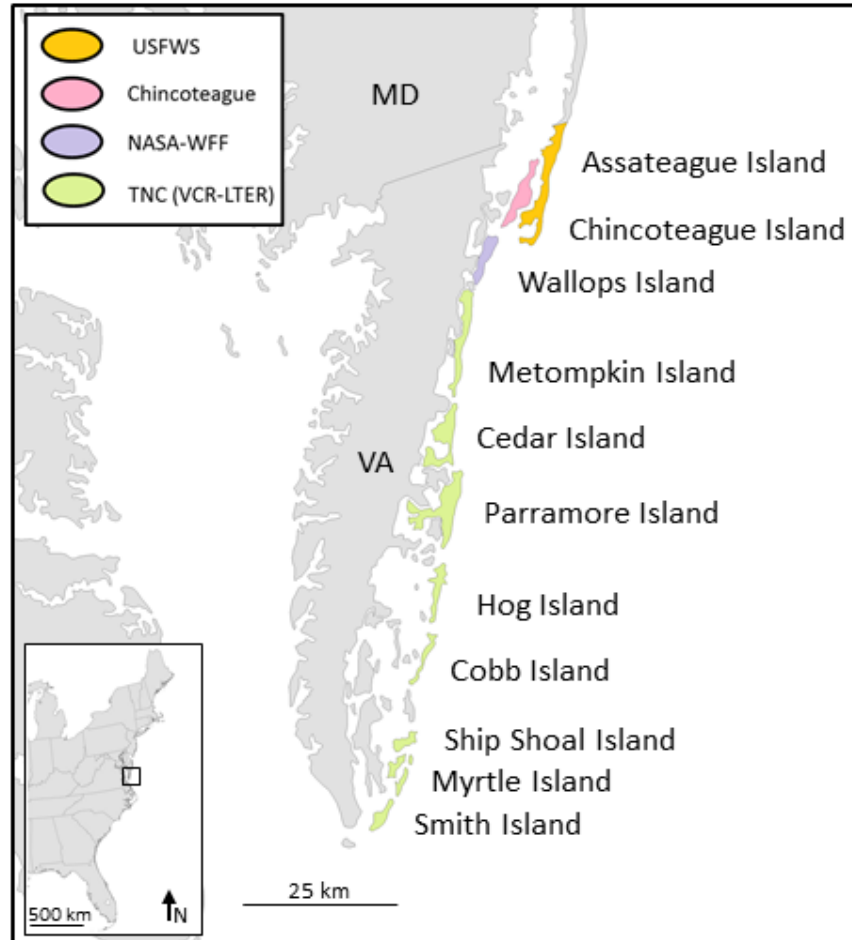


Figure 1. The Virginia Eastern Shore on the U.S. Mid-Atlantic Coast consists of a series of barrier islands owned by different organizations, each with its own management goal: United States Fish and Wildlife (USFWS); the town of Chincoteague, National Aeronautics and Space Administration-Wallops Flight Facility (WFF); The Nature Conservancy (TNC), home to the Virginia Coast Long-term Ecological Research (VCR-LTER) Site.

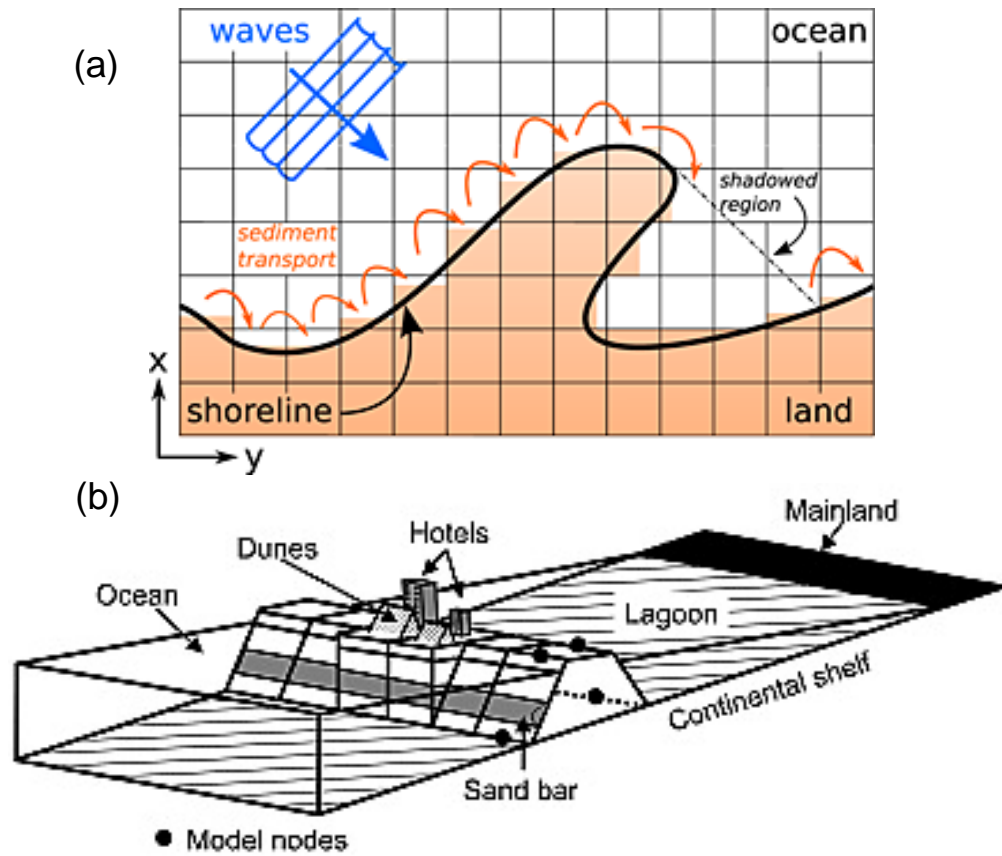


Figure 2. (a) Schematic illustrating key components of the Coastline Evolution Model (CEM; from Johnson et.al. 2014 and (b) the Barrier Island Model (BIM; from McNamara and Werner 2008a).

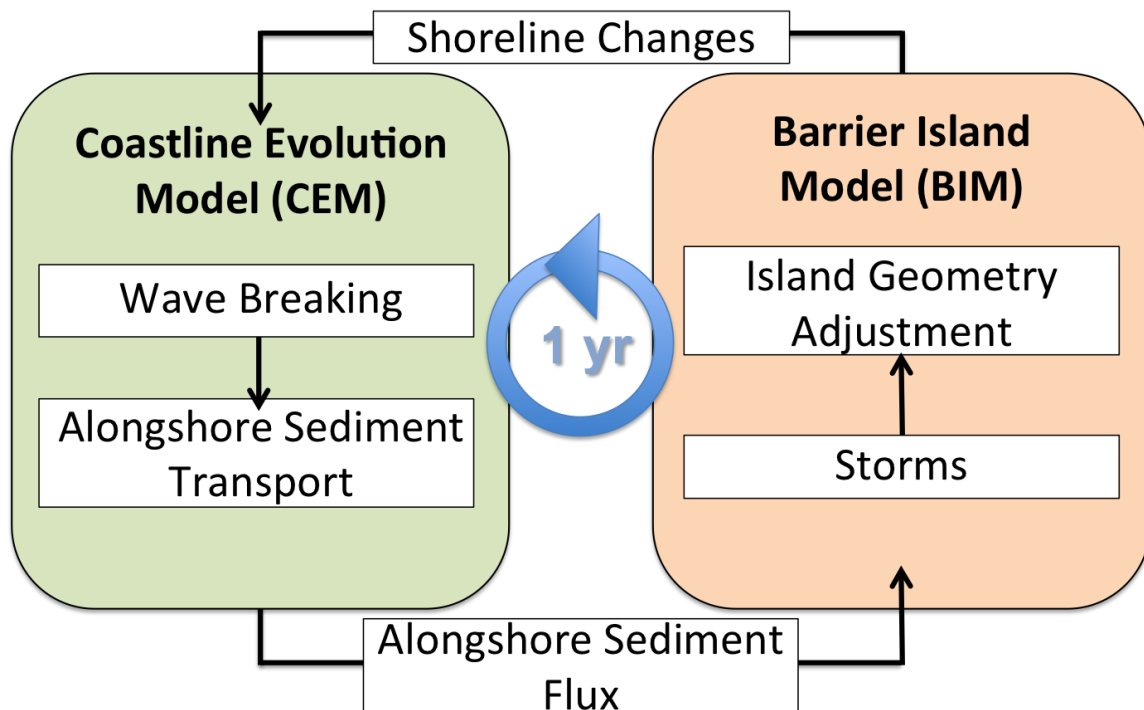


Figure 3. Flow diagram illustrating the factors accounted for by Coastline Evolution Model (CEM) and the Barrier Island Model (BIM) and the parameters that are passed between them as they have been coupled to create the Barrier Island and Inlet Modeling System (BIIMS).

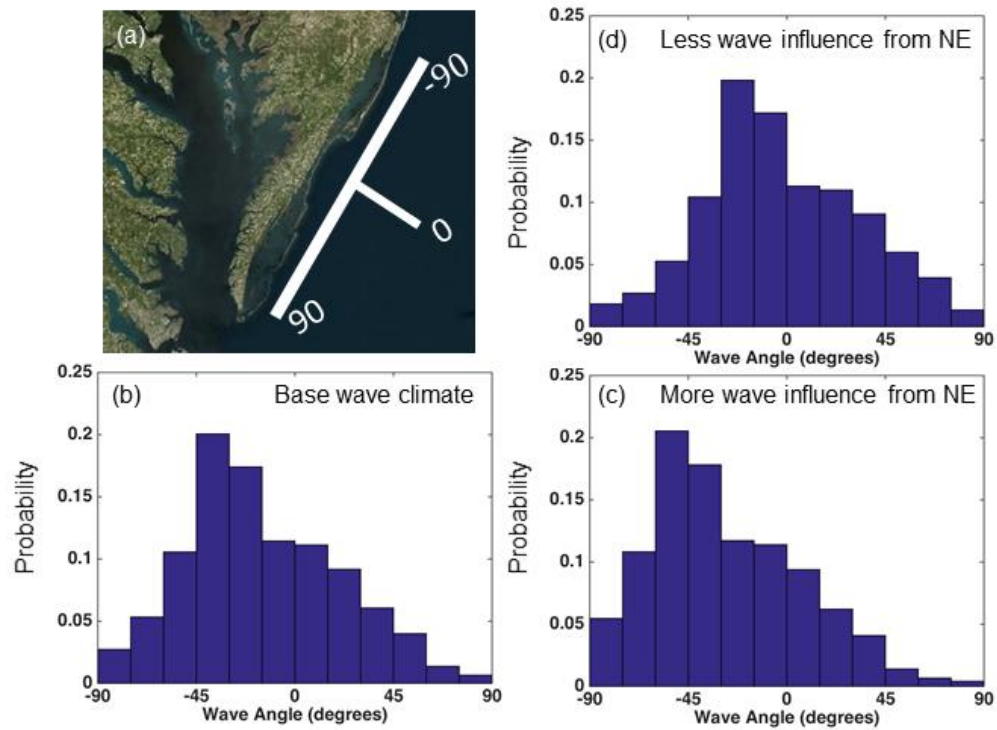


Figure 4. Wave climate distributions. Negative wave angles indicate waves approaching from the E and NE. (a) wave angle of 0° indicates waves approaching perpendicular to the general coastline trend (b) standard wave climate based on Wave Information Studies (WIS) (c) wave climate representing a greater proportion of waves derived from hurricanes (d) wave climate representing a lesser proportion of waves derived from hurricanes.

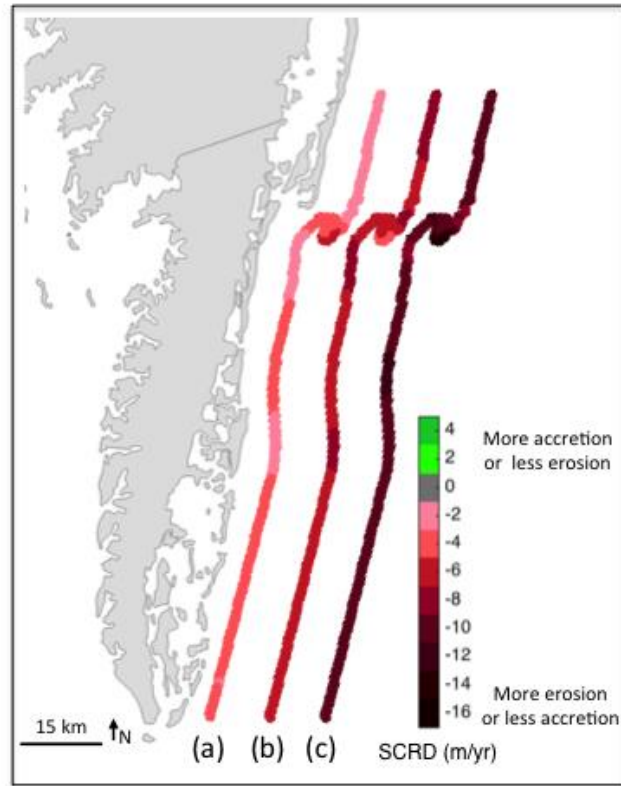


Figure 5. Relative sea level rise (RSLR) scenarios. Negative shoreline change rate differences (SCRD) for the (a) Low, (b) High, (c) Highest scenarios indicate more erosion or less accretion relative to the base case.

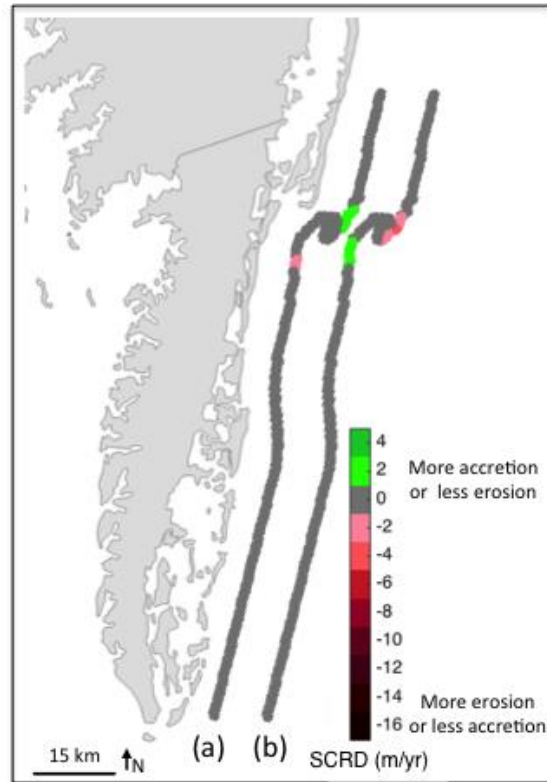


Figure 6. Wave climate change scenarios. Negative shoreline change rate differences (SCRD) indicate more erosion or less accretion relative to the base case. (a) A greater proportion of waves approaching from the NE increases erosion in the portion of the domain representing Wallops Island relative to the base case (b) A lesser proportion of waves approaching from the NE increases erosion in the portion of the domain representing Assateague island relative to the base case.

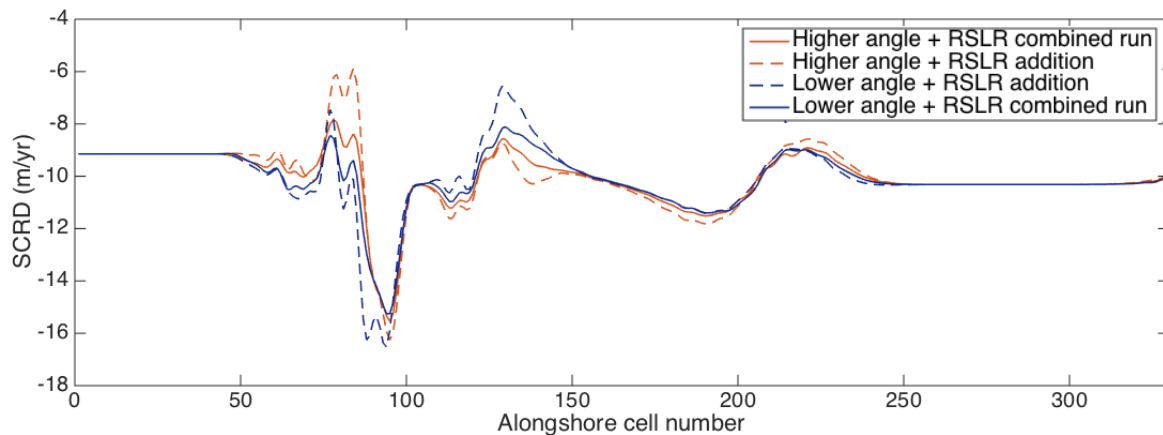


Figure 7. Comparison between modeled combinations of climate scenarios and addition of individual climate scenarios illustrating that in areas with higher rates of erosion relative to the rest of the domain (notably the portion of the domain representing Assateague Island for the higher angle wave climate scenario, shown in orange or the portion of the domain representing Wallops Island for the lower angle wave climate scenario, shown in blue) adding individual climate scenarios tends to under predict the amount of negative SCRD. Each alongshore cell is approximately 0.5 km in length.

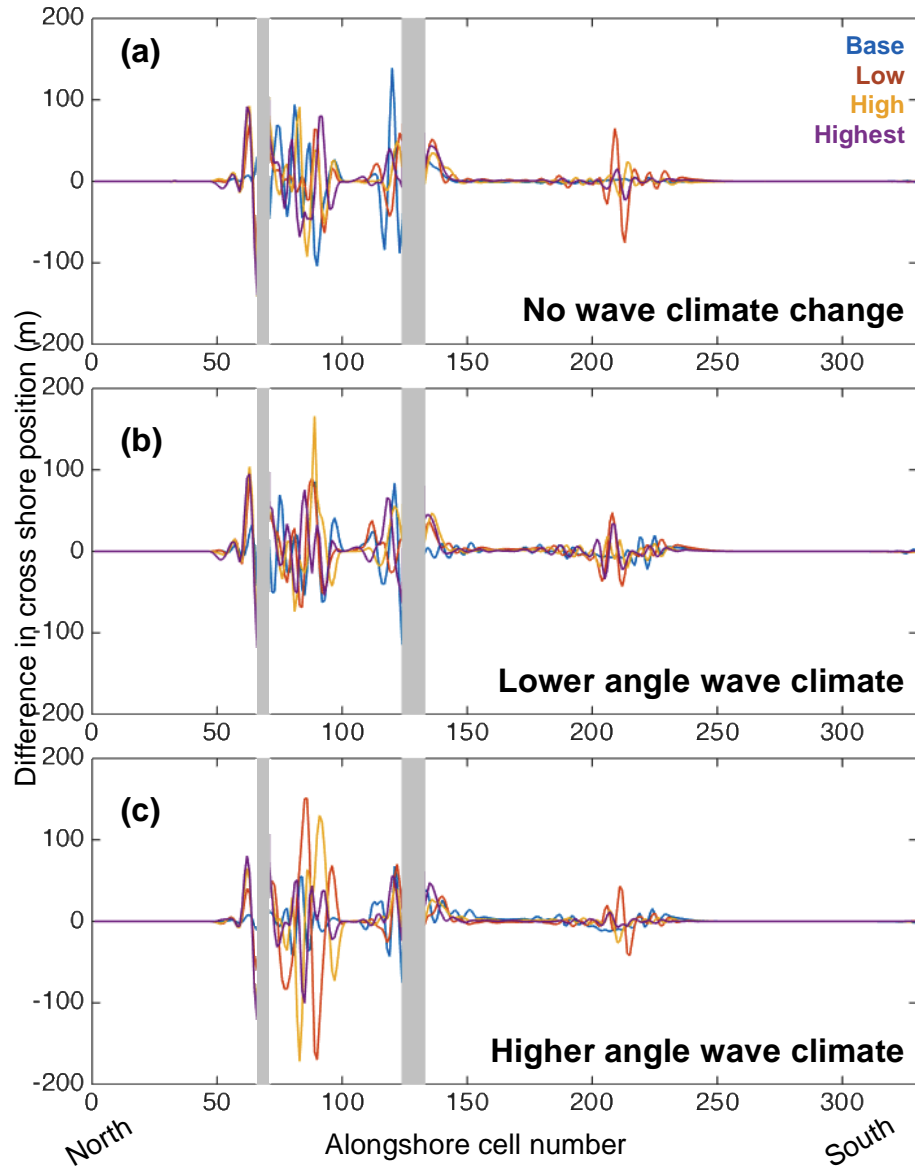


Figure 8. Total differences in cross-shore coastline position between each climate scenario with nourishment and without nourishment after 50 years for (a) lower angle wave climate (a lesser proportion of waves approaching from the NE), (b) a higher angle wave climate (a greater proportion of wave approaching from the NE), and (c) no change in wave climate. Grey bars indicate nourishment zones. Each alongshore cell is approximately 0.5 km in length. A positive difference in cross-shore position indicates that the nourishment scenario is associated with more accretion or less erosion of the coastline relative to the same scenario without nourishment. Across all experiments nourishment produces a positive difference extending only 1-2 km from the nourishment zone. Spikes appearing between nourishment zones do not align across scenarios, arise from stochastic effects related to model discretization, and are not considered effects of nourishment.

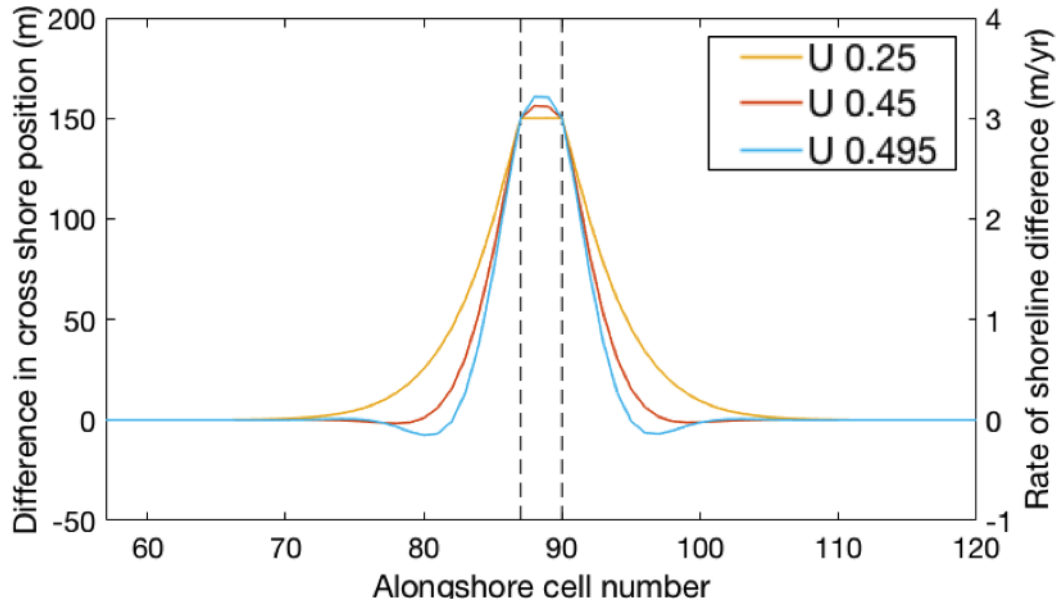


Figure 9. Experiments with the Coastline Evolution Model (CEM) alone show that as waves approach a balance between diffusive and anti-diffusive effects, nourishment effects are more localized alongshore. The parameter U defines the relative influences from high- and low-angle waves, with $U = 0$ corresponding with all low-angle waves, and $U = 0.5$ indicating a balance between low and high-angle influences. Dashed lines indicate the boundaries of the nourishment zone.

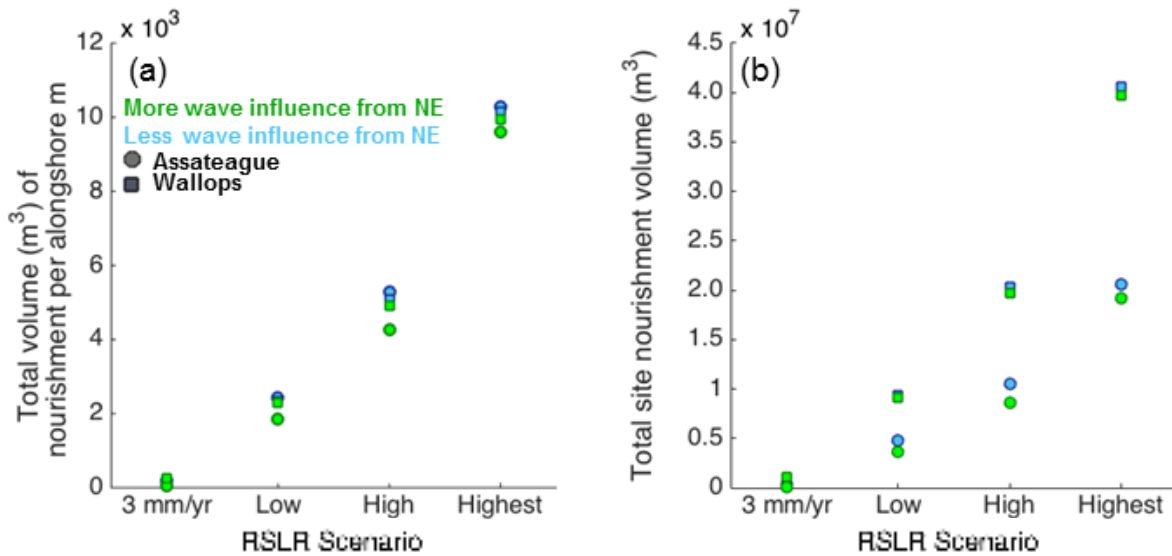


Figure 10. As Relative Sea Level Rise (RSLR) increases, the volume of nourishment sand required to maintain coastline position over 50 model years increases. (a) A lesser proportion of waves approaching from the Northeast (NE, shown in blue) decreases the total volume of nourishment needed per alongshore meter in the portion of the domain representing Wallops Island relative to the portion of the domain representing Assateague Island. A greater proportion of waves approaching from the NE (shown in green) increases erosion in the portion of the domain representing Wallops Island resulting in greater volumes of nourishment needed in this portion of the domain relative to the portion of the domain representing Assateague Island. (b) Regardless of wave climate or RSLR scenario, nourishing the portion of the domain representing Wallops Island (4 km alongshore length) requires roughly twice the total volume of nourishment relative to the Assateague Island nourishment zone (2 km alongshore length) simply because its alongshore length is nearly twice as long.

APPENDIX A: WAVE CLIMATE ANALYSIS

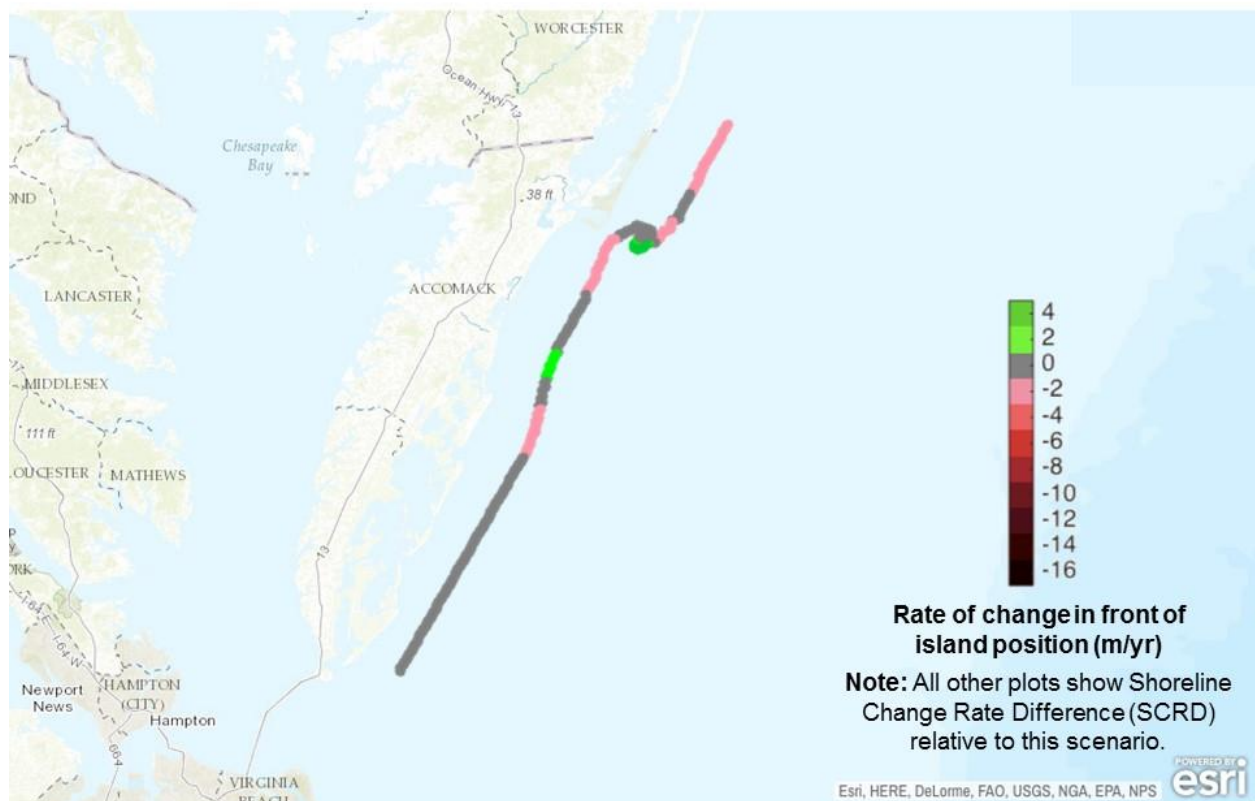
I downloaded the Version 3 time series wave data from Wave Information Studies (WIS) station 63177 (depth of 25m) in November 2015. (Products are available at <http://wis.usace.army.mil/>). These data are hindcasts of mean wave direction, significant wave height, period (among other attributes) at one hour intervals from January 1980 to December 2012. WIS provides mean wave direction in degrees clockwise from true north. To calculate the wave directions relative to the VA coast, I estimated a coastline trend normal of $\sim 118^\circ$ based on satellite images. For each WIS data point, I calculated the proportion of wave influence from each relative angle (E) using the following equation (see Ashton and Murray 2006 a/b): $E = T^{(1/5)} \cdot H^{(12/5)}$, where T is the wave period and H is the significant wave height. I normalized these to create a probability density function binned into 15° bins.

APPENDIX B: SCRD AND INLET RESULTS FOR ALL EXPERIMENTS

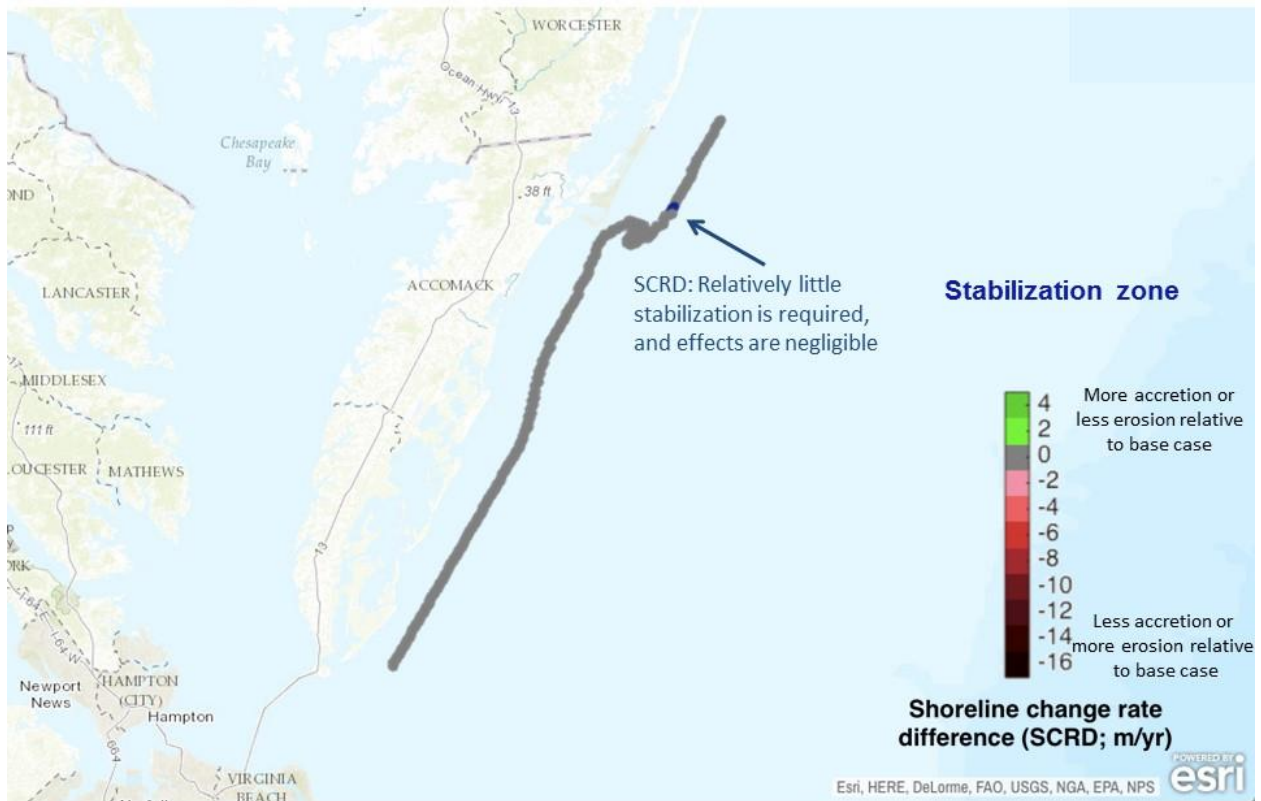
Summary of Scenarios

Group #	Title	Description	# of Runs
1	Base case	3 mm/yr background SLR	1
2	Stabilization Only	2km at Assateague only, 4km at Wallops only, both sites	3
3	Sea Level Rise Only	Low, High, and Highest Scenarios	3
4	Wave Climate Change Only	Greater proportion of wave influence from NE, Lesser proportion of wave influence from NE	2
5	Sea Level Rise + Wave Climate Change		6
6	Stabilization + Wave Climate Change		6
7	Stabilization + Sea Level Rise		9
8	Stabilization + Sea Level Rise + Wave Climate Change		18
			Total: 48

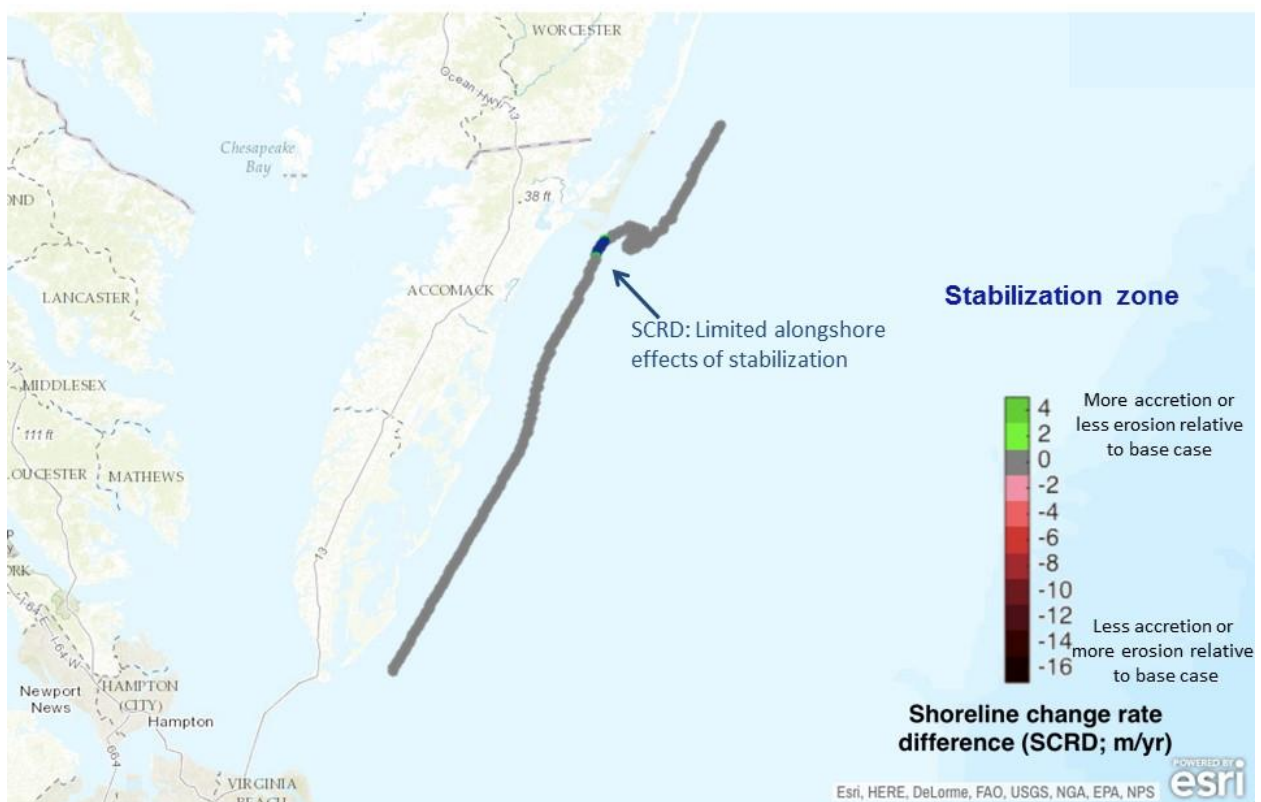
1-1 Base Case



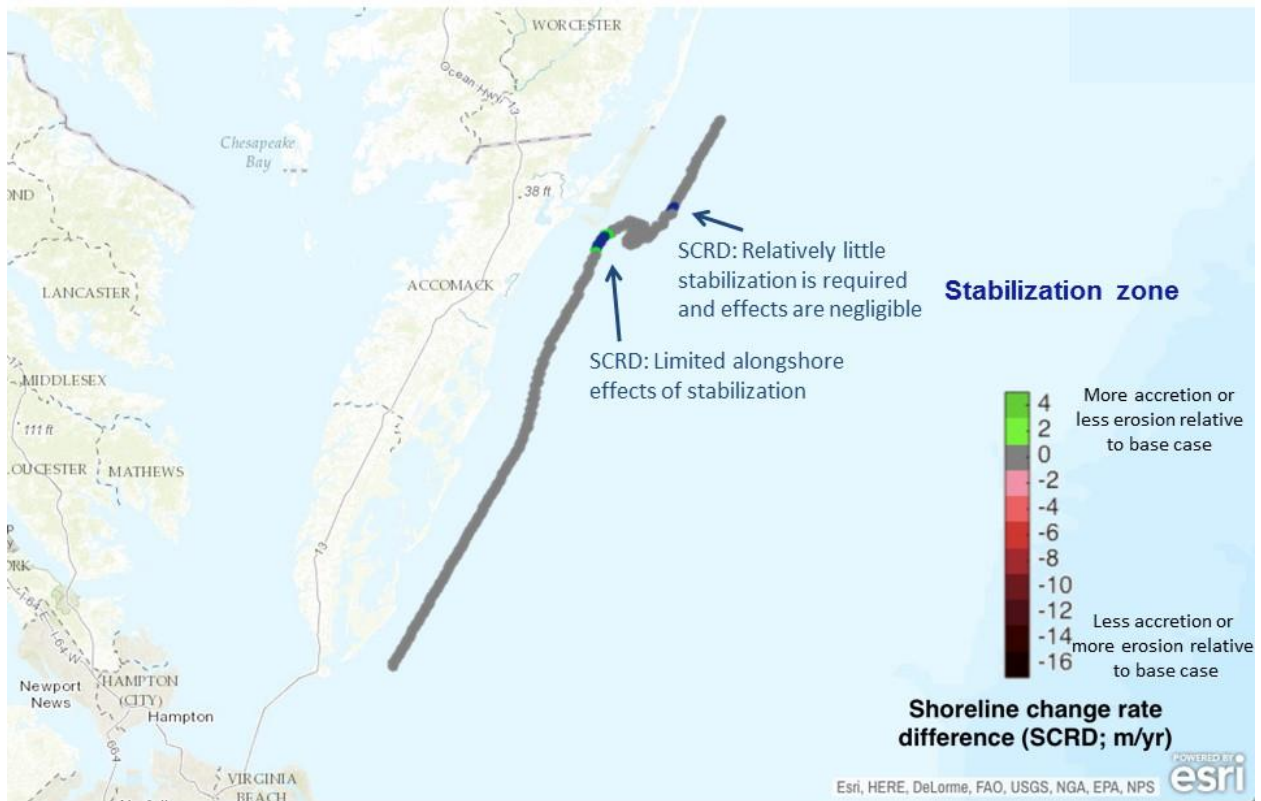
2-1 Stabilize Assateague



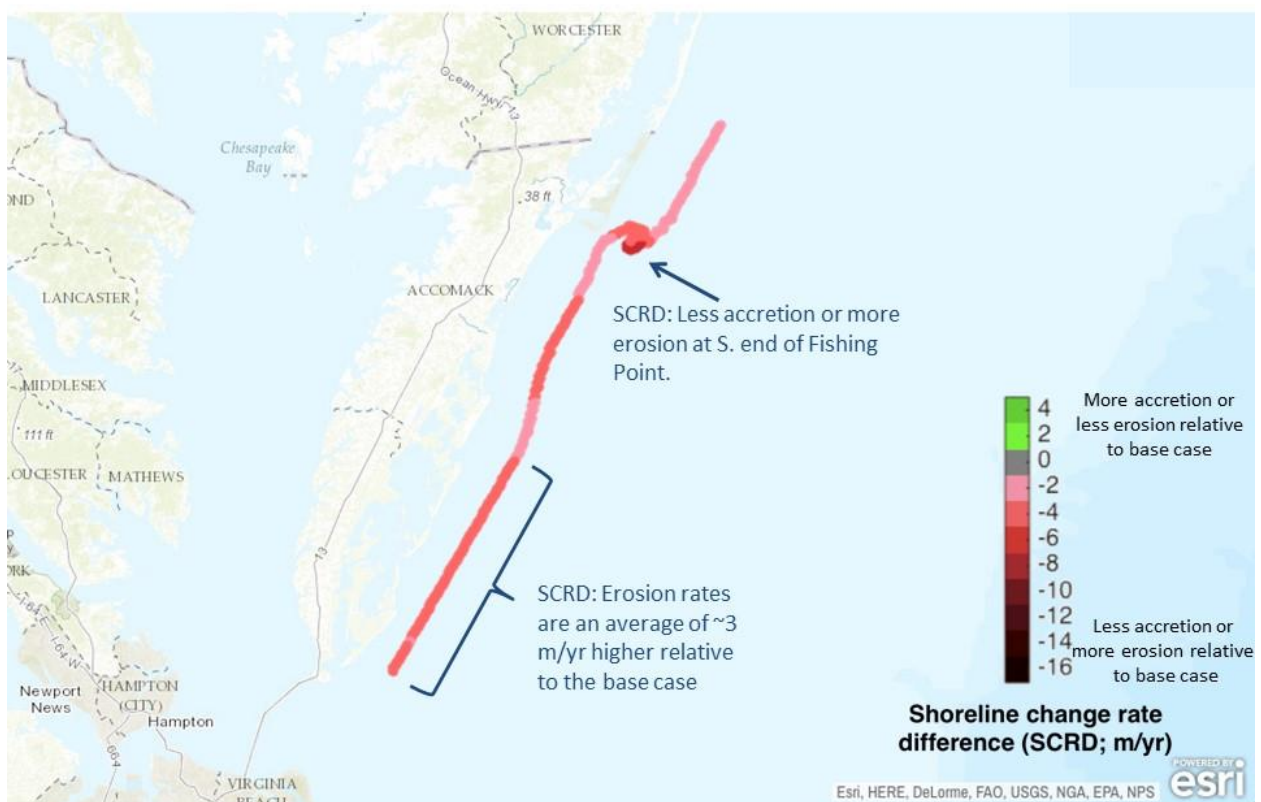
2-2 Stabilize Wallops



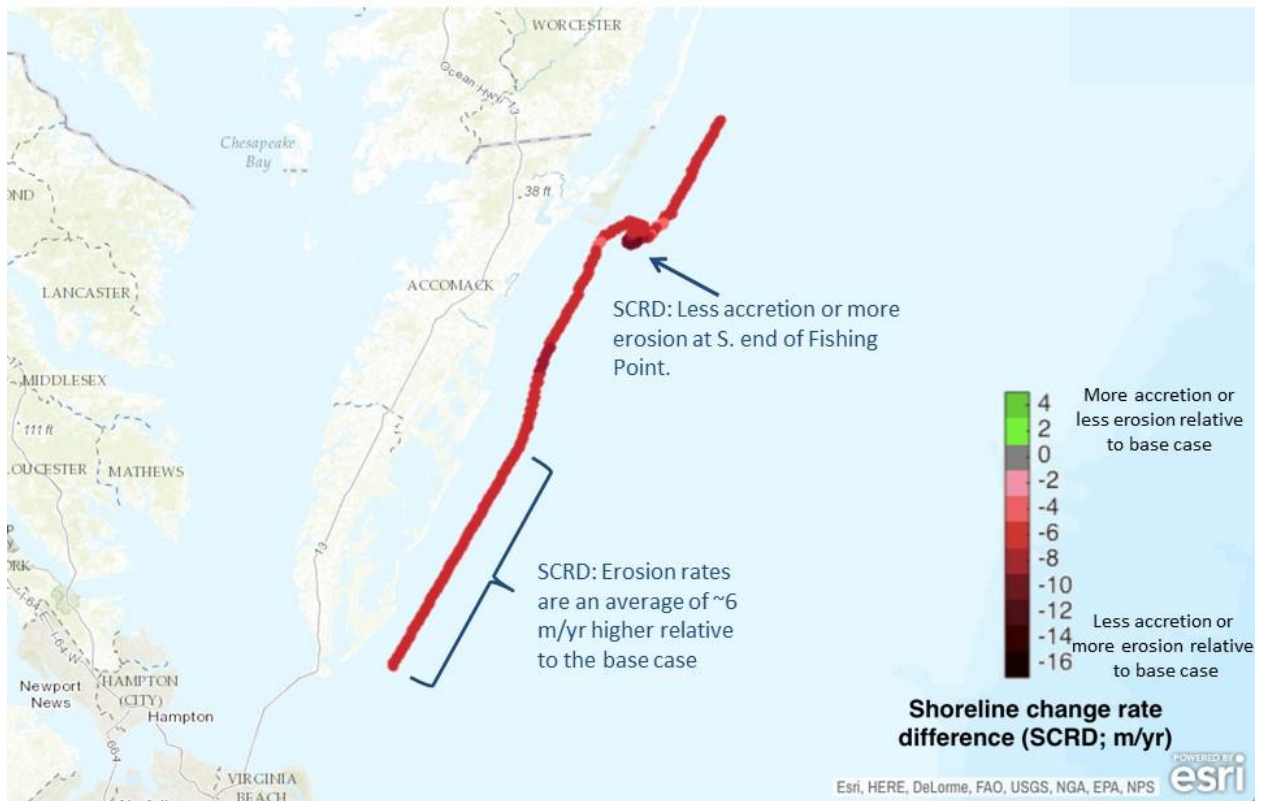
2-3 Stabilize both sites



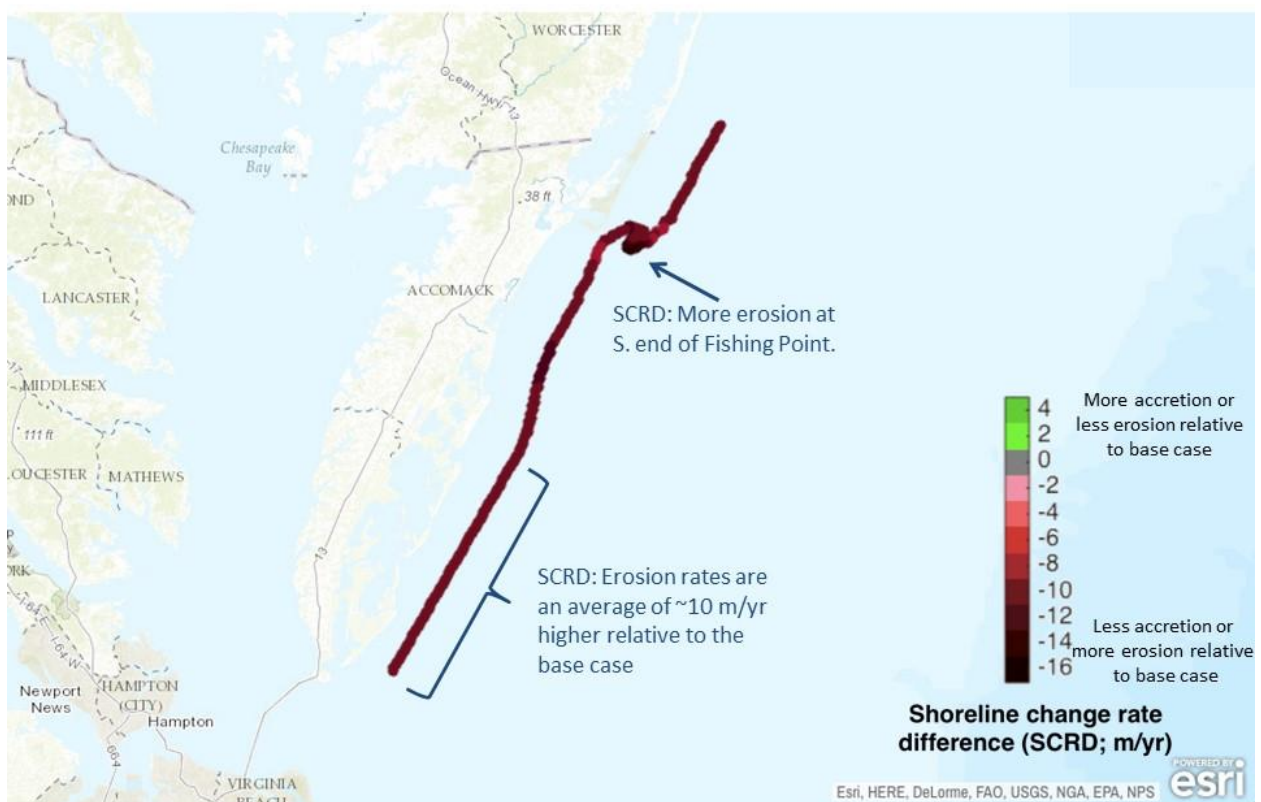
3-1 Low SLR

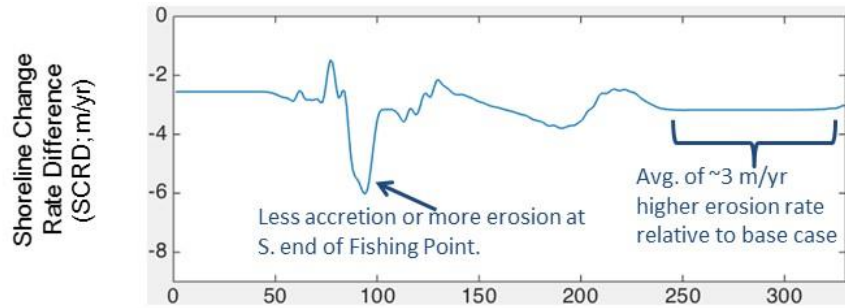


3-2 High SLR

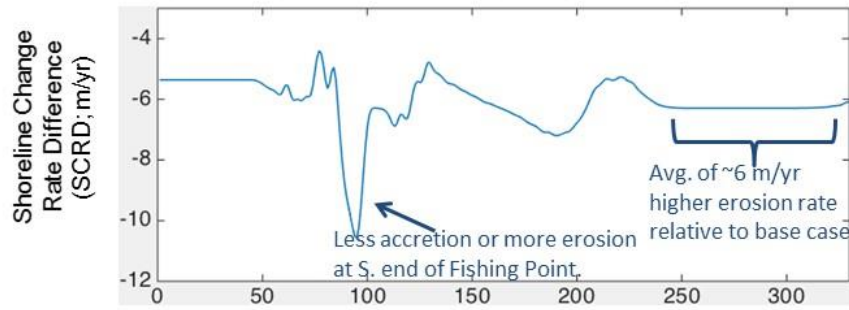


3-3 Highest SLR

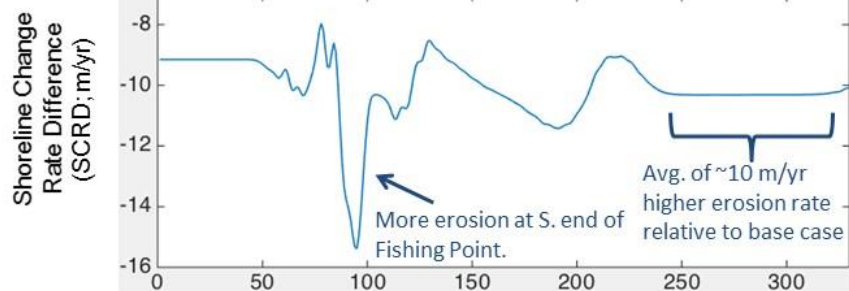




3-1 Low SLR



3-2 High SLR



3-3 Highest SLR

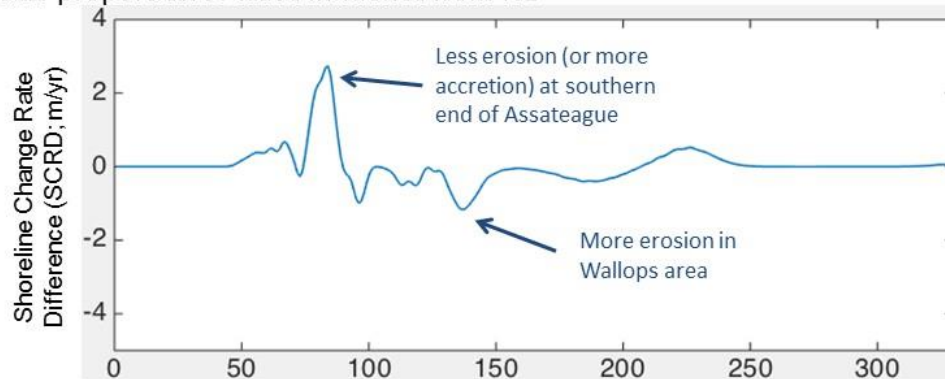
4-1 Greater proportion of wave influence from NE



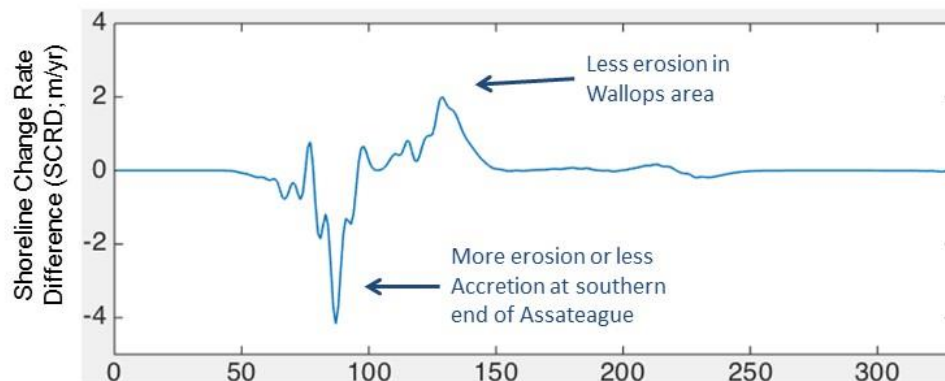
4-2 Lesser proportion of wave influence from NE



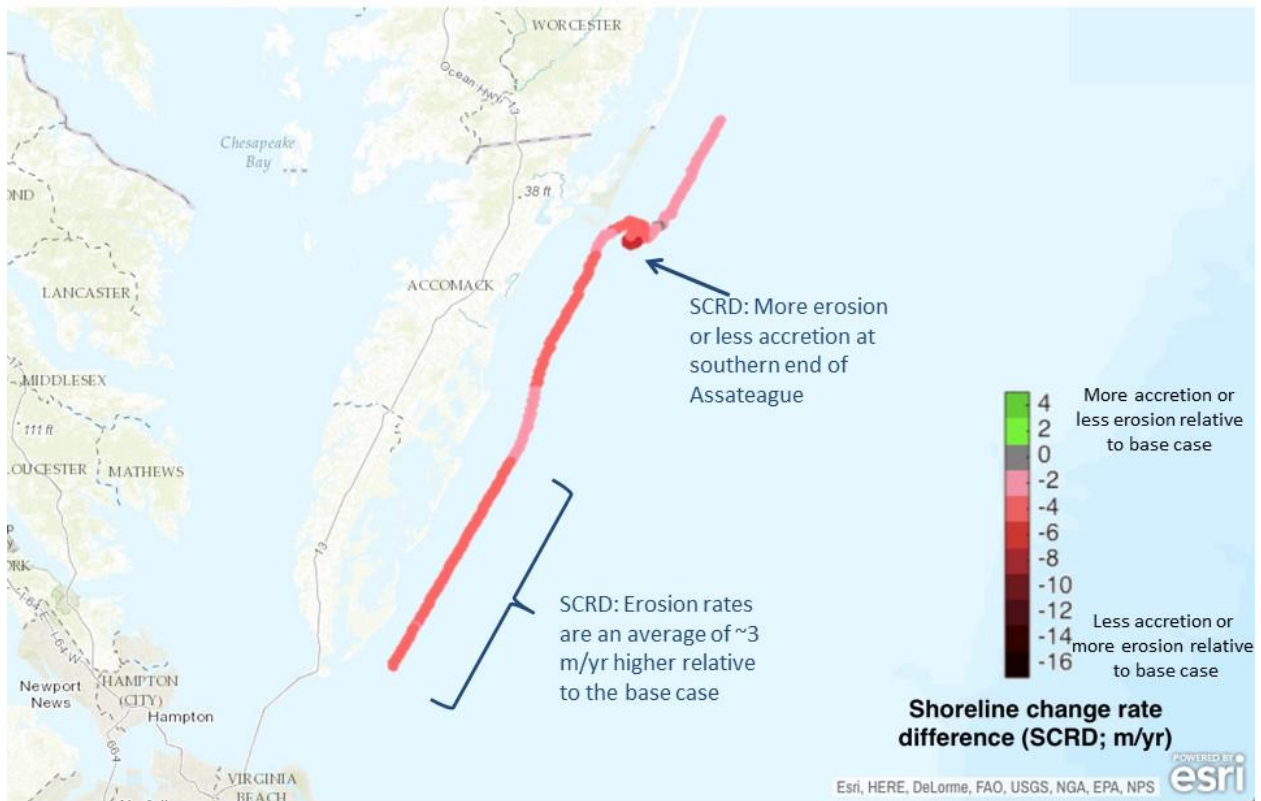
4-1 Greater proportion of wave influence from NE



4-2 Lesser proportion of wave influence from NE



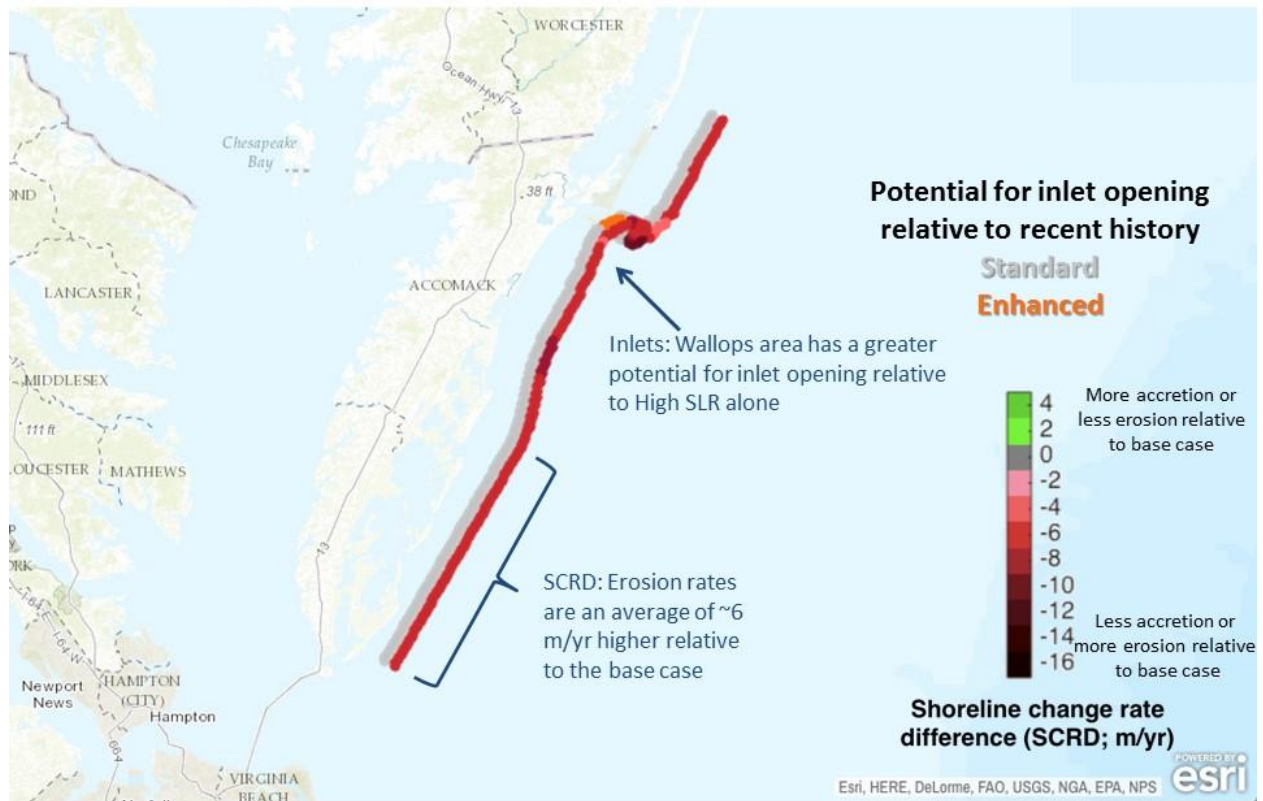
5-1 Low SLR + Greater proportion of wave influence from NE



5-2 Low SLR + Lesser proportion of wave influence from NE



5-3 High SLR + Greater proportion of wave influence from NE



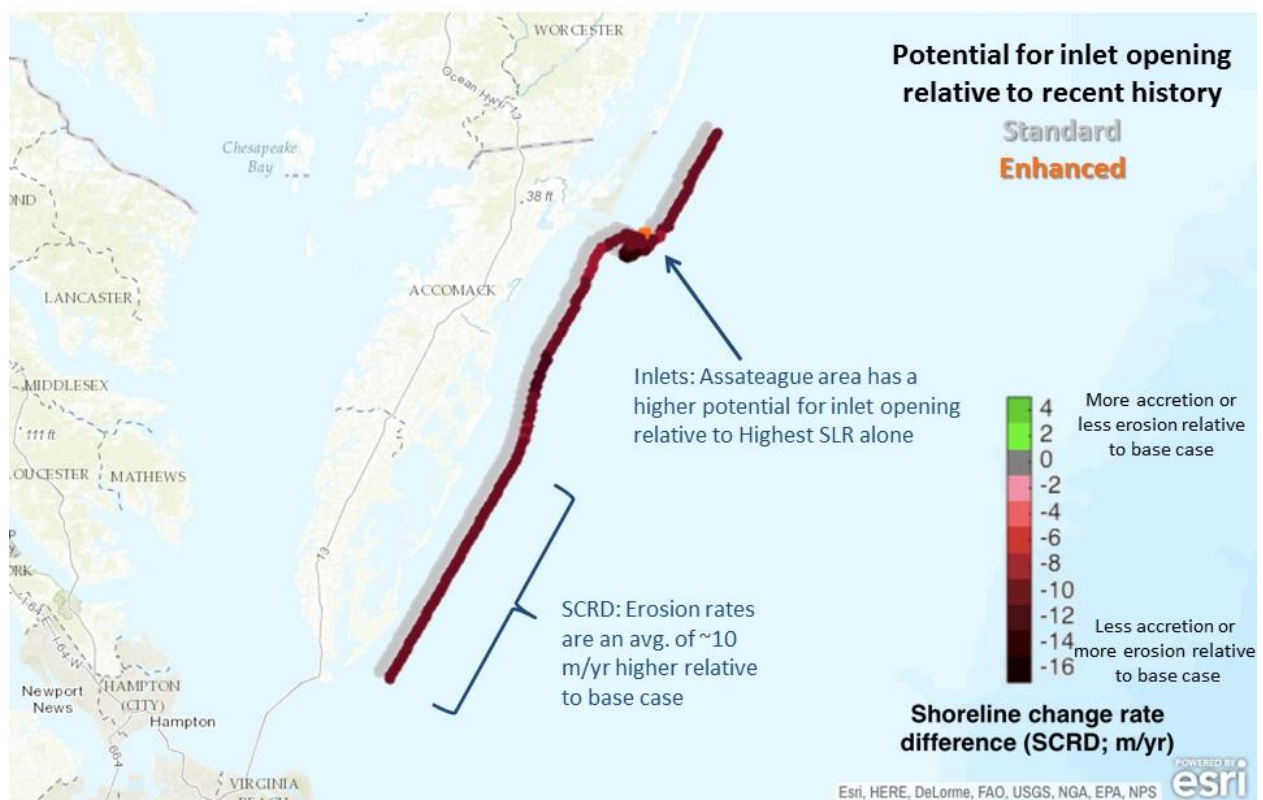
5-4 High SLR + Lesser proportion of wave influence from NE



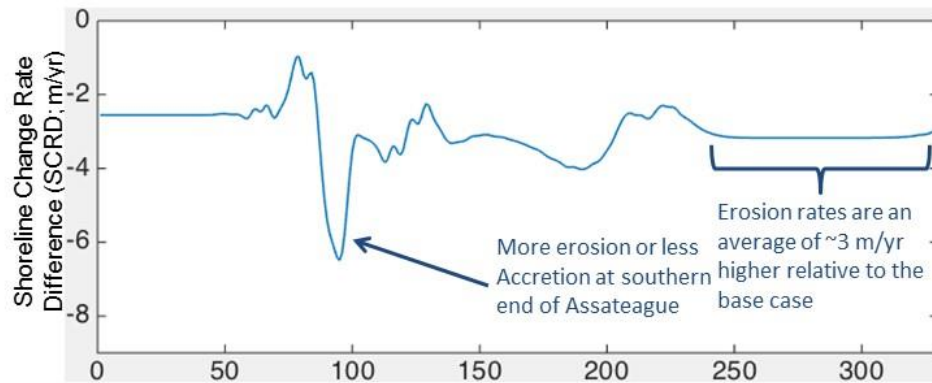
5-5 Highest SLR + Greater proportion of wave influence from NE



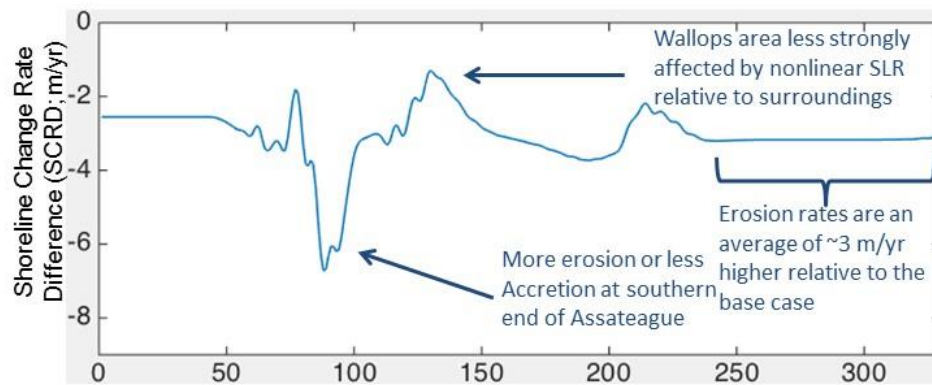
5-6 Highest SLR + Lesser proportion of wave influence from NE



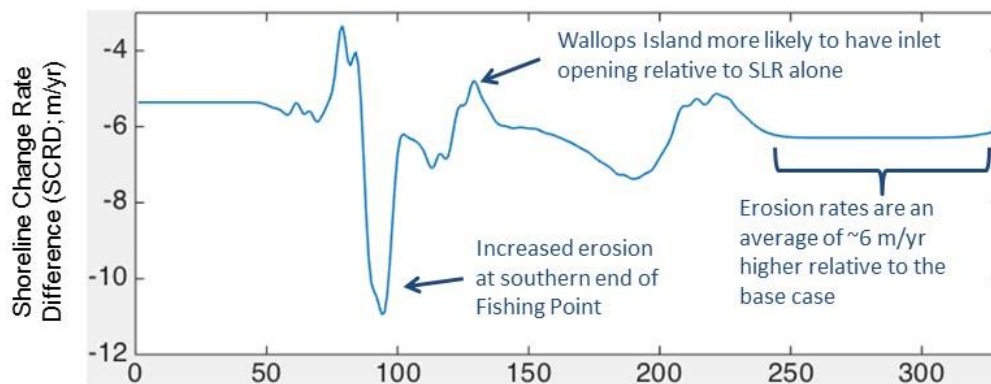
5-1 Low SLR + Greater proportion of wave influence from NE



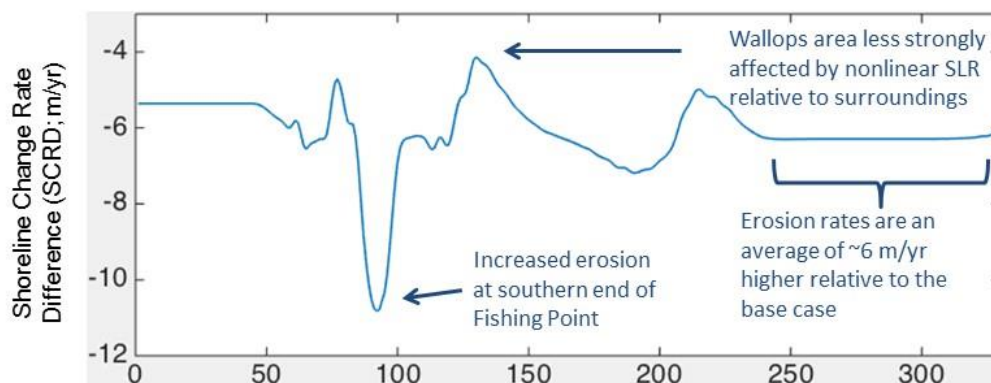
5-2 Low SLR + Lesser proportion of wave influence from NE



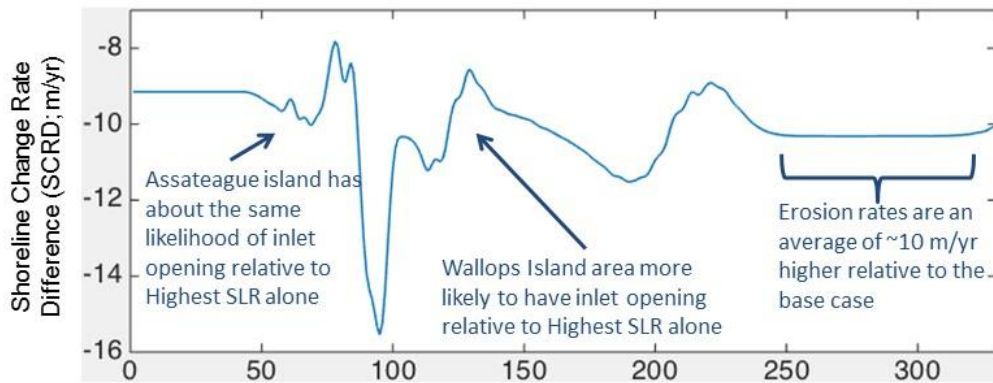
5-3 High SLR + Greater proportion of wave influence from NE



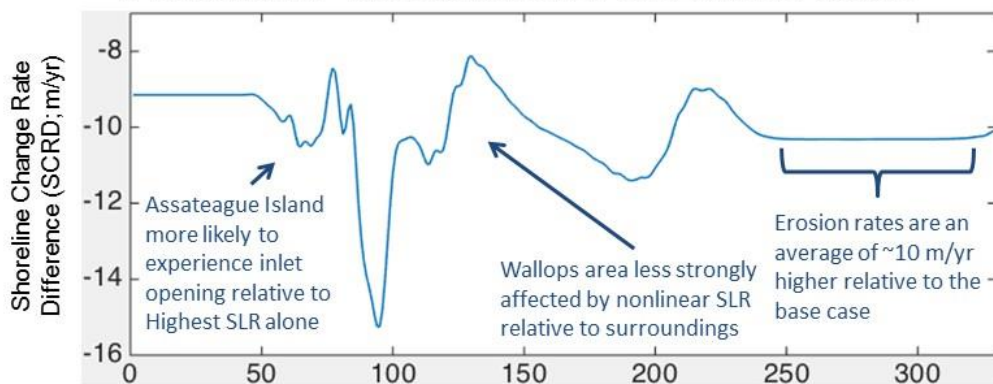
5-4 High SLR + Lesser proportion of wave influence from NE



5-5 Highest SLR + Greater proportion of wave influence from NE



5-6 Highest SLR + Lesser proportion of wave influence from NE



6-1 Stabilize Assateague + Greater proportion of wave influence from NE



6-2 Stabilize Wallops + Greater proportion of wave influence from NE



6-3 Stabilize both sites + Greater proportion of wave influence from NE



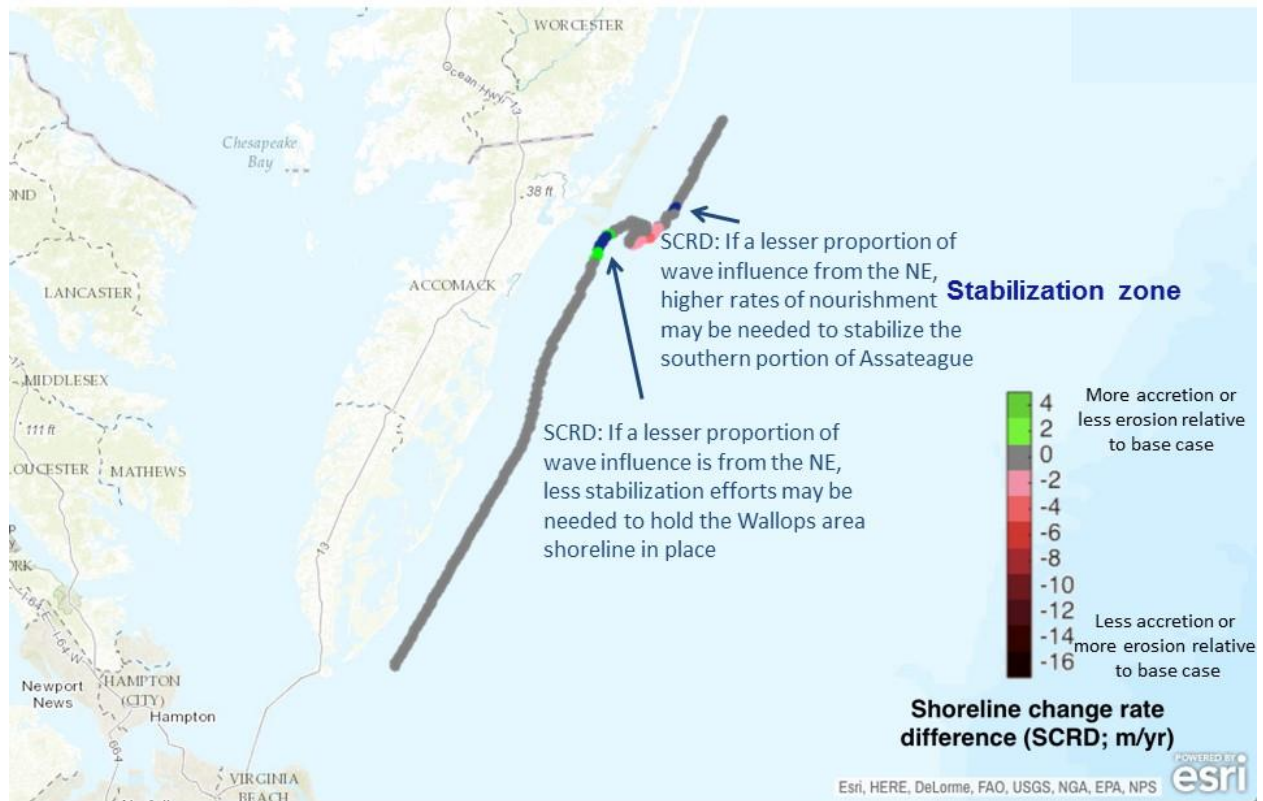
6-4 Stabilize Assateague + Lesser proportion of wave influence from NE (15°)



6-5 Stabilize Wallops + Lesser proportion of wave influence from NE (15°)



6-6 Stabilize both sites + Lesser proportion of wave influence from NE (15°)



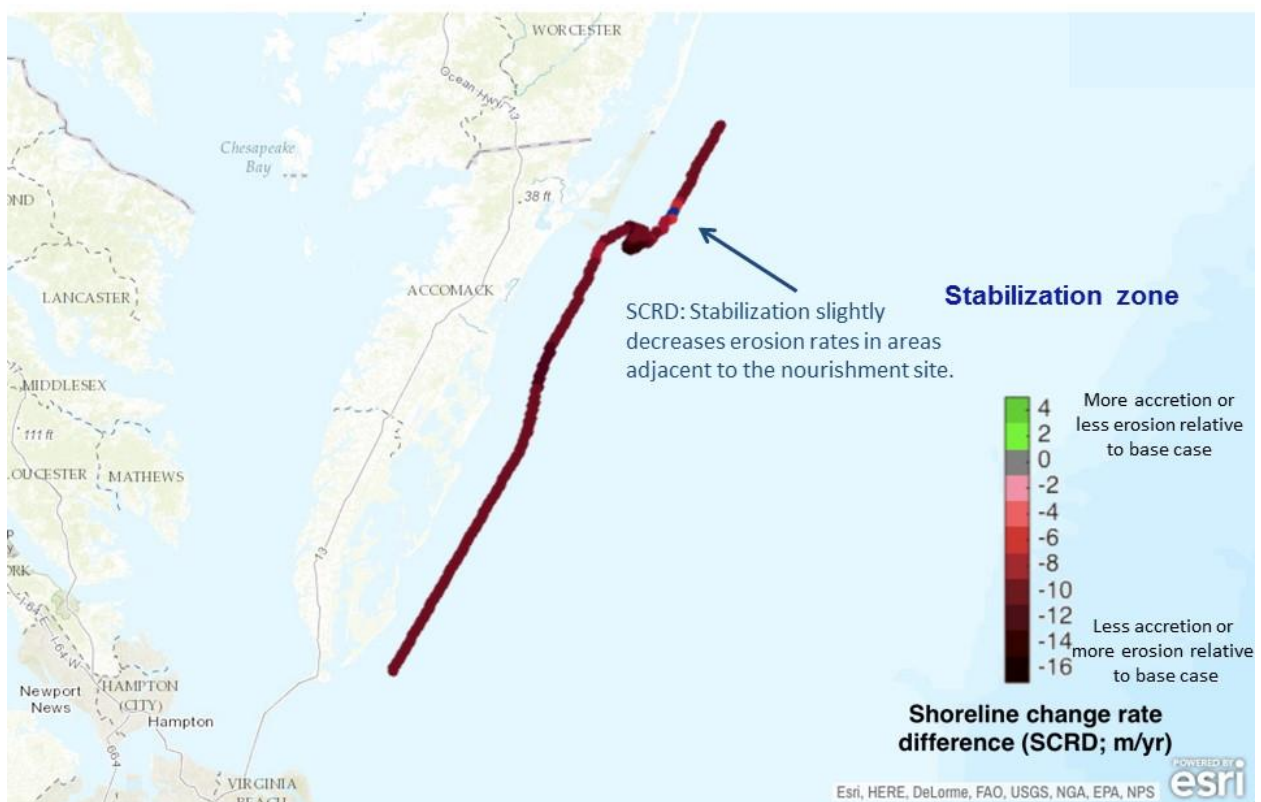
7-1 Stabilize Assateague + Low SLR



7-2 Stabilize Assateague + High SLR



7-3 Stabilize Assateague + Highest SLR



7-4 Stabilize Wallops + Low SLR



7-5 Stabilize Wallops + High SLR



7-6 Stabilize Wallops + Highest SLR



7-7 Stabilize both sites + Low SLR



7-8 Stabilize both sites + High SLR



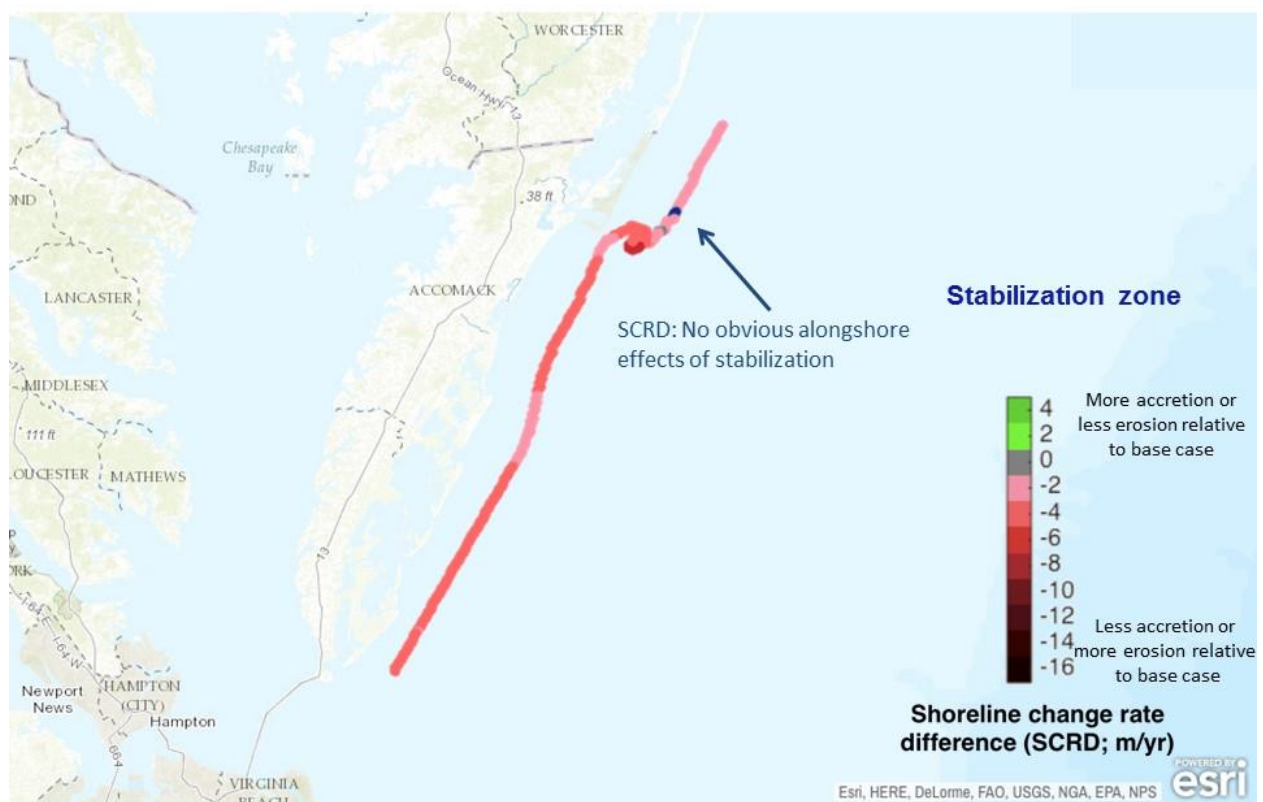
7-9 Stabilize both sites + Highest SLR



8-1 Stabilize Assateague + Low SLR + Greater proportion of wave influence from NE (15°)



8-2 Stabilize Assateague + Low SLR + Lesser proportion of wave influence from NE



8-3 Stabilize Assateague + High SLR + Greater proportion of wave influence from NE



8-4 Stabilize Assateague + High SLR + Lesser proportion of wave influence from NE (15°)



8-5 Stabilize Assateague + Highest SLR + Greater proportion of wave influence from NE (15°)



8-6 Stabilize Assateague + Highest SLR + Lesser proportion of wave influence from NE (15°)



8-7 Stabilize Wallops + Low SLR + Greater proportion of wave influence from NE (15°)



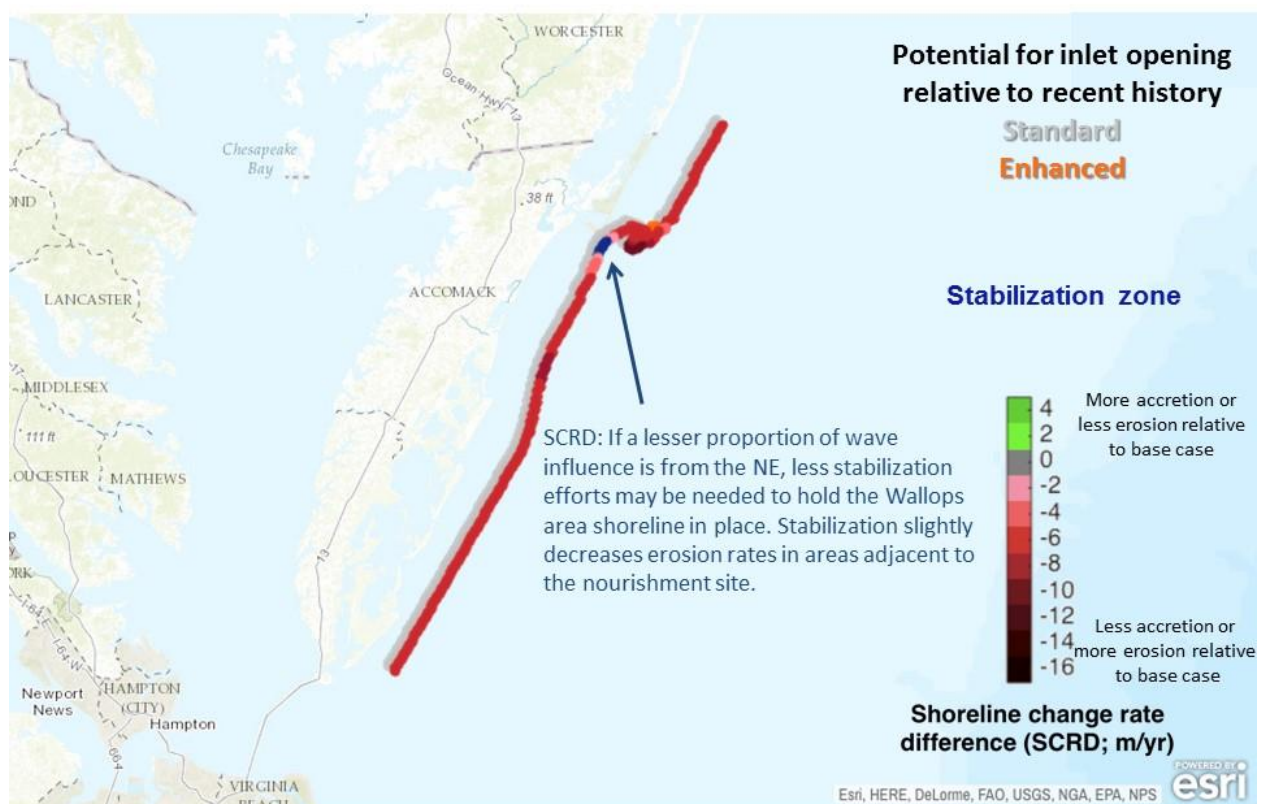
8-8 Stabilize Wallops + Low SLR + Lesser proportion of wave influence from NE (15°)



8-9 Stabilize Wallops+ High SLR + Greater proportion of wave influence from NE (15°)



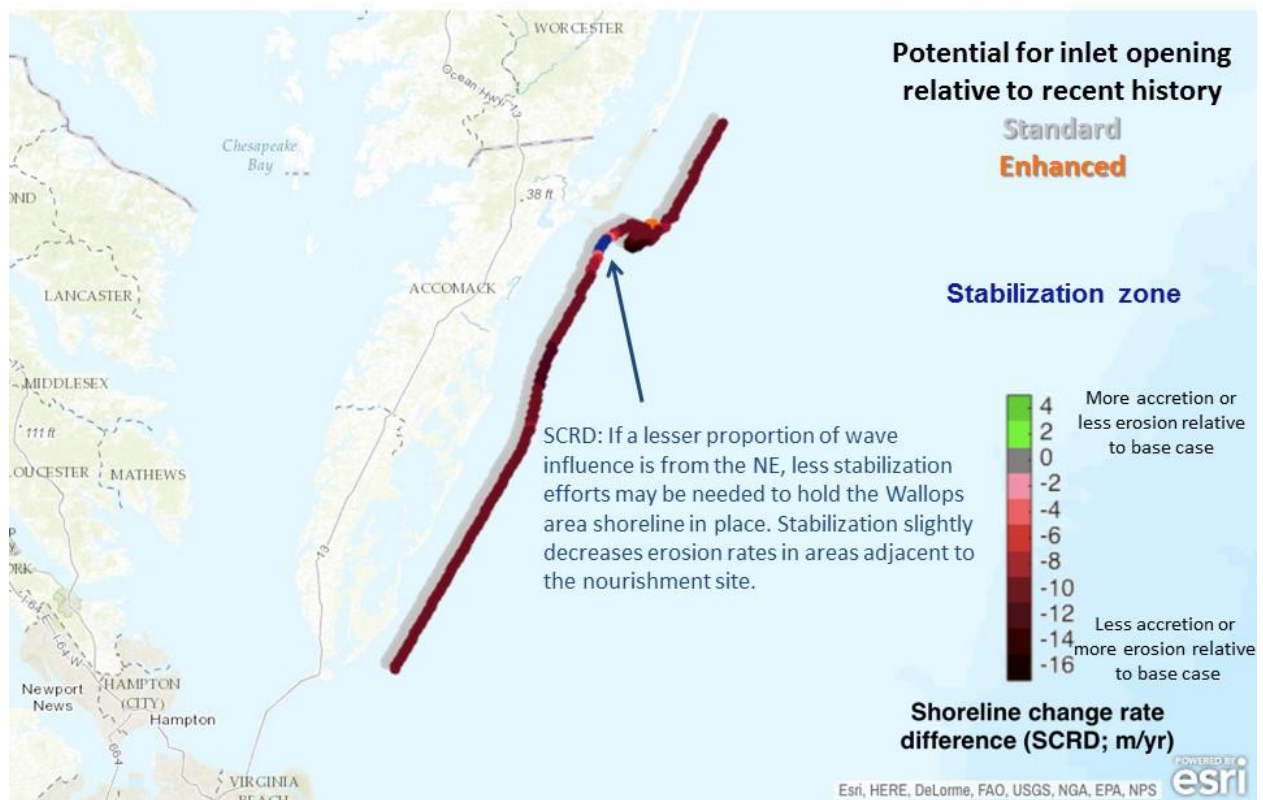
8-10 Stabilize Wallops + High SLR + Lesser proportion of wave influence from NE (15°)



8-11 Stabilize Wallops + Highest SLR + Greater proportion of wave influence from NE



8-12 Stabilize Wallops + Highest SLR + Lesser proportion of wave influence from NE



8-13 Stabilize both sites + Low SLR + Greater proportion of wave influence from NE



8-14 Stabilize both sites + Low SLR + Lesser proportion of wave influence from NE (15°)



8-15 Stabilize both sites + High SLR + Greater proportion of wave influence from NE (15°)



8-16 Stabilize both sites + High SLR + Lesser proportion of wave influence from NE (15°)



8-17 Stabilize both sites + Highest SLR + Greater proportion of wave influence from NE (15°)



8-18 Stabilize both sites + Highest SLR + Lesser proportion of wave influence from NE (15°)



REFERENCES

- Accomack-Northampton Planning District Commission, 2014. Community Leader Workshop Summary Report.
- Allen, M.R., Barros, V.R., Broome, J., Cramer, W., Christ, R., Church, J.A., Clarke, L., 2014. IPCC Fifth Assessment Synthesis Report-Climate Change 2014 Synthesis Report. IPCC Fifth Assess. Synth. Report-Climate Chang. 2014 Synth. Rep.
- Ashton, a, Murray, a B., Arnault, O., 2001. Formation of coastline features by large-scale instabilities induced by high-angle waves. *Nature* 414, 296–300. doi:10.1038/35104541
- Ashton, A.D., Murray, a B., 2006a. High-angle wave instability and emergent shoreline shapes: 1. Modeling of sand waves, flying spits, and capes. *J. Geophys. Res.* 111, F04011. doi:10.1029/2005JF000422
- Ashton, A.D., Murray, a B., 2006b. High-angle wave instability and emergent shoreline shapes: 2. Wave climate analysis and comparisons to nature. *J. Geophys. Res. F Earth Surf.* 111, F04012. doi:10.1029/2005JF000423
- Ashton, A.D., Nienhuis, J., Ells, K., 2016. On a neck, on a spit: Controls on the shape of free spits. *Earth Surf. Dyn.* 4, 193–210. doi:10.5194/esurf-4-193-2016
- Bruun, P., 1962. Sea-Level Rise as a Cause of Shore Erosion, in: *Proceedings of the American Society of Civil Engineers*. pp. 117–130.
- Cowell, P. J., Roy, P. S., & Jones, R. A. (1995). Simulation of large-scale coastal change using a morphological behaviour model. *Marine Geology*, 126(1), 45-61.
- Ells, K., Murray, A.B., 2012. Long-term, non-local coastline responses to local shoreline stabilization. *Geophys. Res. Lett.* 39. doi:10.1029/2012GL052627
- Emanuel, K.A., 2013. Downscaling CMIP5 climate models shows increased tropical cyclone activity over the 21st century. *Proc. Natl. Acad. Sci. U. S. A.* 110, 12219–24. doi:10.1073/pnas.1301293110
- FitzGerald, D.M., Fenster, M.S., Argow, B. a., Buynevich, I. V., 2008. Coastal Impacts Due to Sea-Level Rise. *Annu. Rev. Earth Planet. Sci.* 36, 601–647. doi:10.1146/annurev.earth.35.031306.140139
- Galgano, F.A., Leatherman, S.P., 2005. Modes and Patterns of Shoreline Change, in: Schwartz, M.L. (Ed.), *Encyclopedia of Coastal Science*. Springer Netherlands, Dordrecht, pp. 651–656. doi:10.1007/1-4020-3880-1_217
- Hapke, C.J., Kratzmann, M.G., Himmelstoss, E.A., 2013. Geomorphic and human influence on large-scale coastal change. *Geomorphology* 199, 160–170. doi:10.1016/j.geomorph.2012.11.025
- Hardaway, C.S., Milligan, D.A., Wilcox, C.A., Smith, C., 2015. Wallops Assateague Chincoteague Inlet (WACI) Geologic and Coastal Management Summary Report.
- Johnson, J.M., Moore, L.J., Ells, K., Murray, A.B., Adams, P.N., Iii, R.A.M., Jaeger, J.M., 2014.

- Recent shifts in coastline change and shoreline stabilization linked to storm climate change. doi:10.1002/esp.3650
- Knutson, T.R., McBride, J.L., Chan, J., Emanuel, K., Holland, G., Landsea, C., Held, I., Kossin, J.P., Srivastava, a. K., Sugi, M., 2010. Tropical cyclones and climate change. *Nat. Geosci.* 3, 157–163. doi:10.1038/ngeo779
- Komar, P.D., Allan, J.C., 2008. Increasing Hurricane-Generated Wave Heights along the U.S. East Coast and Their Climate Controls. *J. Coast. Res.* 242, 479–488. doi:10.2112/07-0894.1
- Lazarus, E., Ashton, A., and Murray, A.B., 2011, Cumulative versus transient shoreline change: Dependencies on temporal and spatial scale, *J. Geophysical Research*, 116, F022014, doi:10.1029/2010JF001835.
- Lazarus, E.D., McNamara, D.E., Smith, M.D., Gopalakrishnan, S., Murray, A.B., 2011. Emergent behavior in a coupled economic and coastline model for beach nourishment. *Nonlinear Process. Geophys.* 18, 989–999. doi:10.5194/npg-18-989-2011
- Leatherman, S.P., Rice, T.E., Goldsmith, V., 1982. Virginia Barrier Island Configuration : A Reappraisal. *Science* (80). 215, 285–287.
- Leatherman, S. P. (1983). Barrier dynamics and landward migration with Holocene sea-level rise. *Nature*, 301, 415–417.
- Lorenzo-Trueba, J., Ashton, A.D., 2014. Rollover, drowning, and discontinuous retreat: Distinct modes of barrier response to sea-level rise arising from a simple morphodynamic model. *J. Geophys. Res. Earth Surf.* 119, 779–801. doi:10.1002/2013JF002941
- McNamara, D.E., Keeler, A., 2013. A coupled physical and economic model of the response of coastal real estate to climate risk. *Nat. Clim. Chang.* 3, 559–562. doi:10.1038/nclimate1826
- McNamara, D.E., Murray, B.A., Smith, M.D., 2011. Coastal sustainability depends on how economic and coastline responses to climate change affect each other. *Geophys. Res. Lett.* 38. doi:10.1029/2011GL047207
- McNamara, D.E., Werner, B.T., 2008a. Coupled barrier island-resort model: 1. Emergent instabilities induced by strong human-landscape interactions. *J. Geophys. Res. F Earth Surf.* 113, F01016. doi:10.1029/2007JF000840
- McNamara, D.E., Werner, B.T., 2008b. Coupled barrier island-resort model: 2. Tests and predictions along Ocean City and Assateague Island National Seashore, Maryland. *J. Geophys. Res. Earth Surf.* 113. doi:10.1029/2007JF000841
- Mitchell, M., Hershner, C., Julie, H., Schatt, D., Mason, P., Eggington, E., 2013. Recurrent Flooding Study for Tidewater Virginia. *Virginia Inst. Mar. Sci. Cent. Coast. Resour. Manag.*
- Moore, L.J., List, J.H., Williams, S.J., Stolper, D., 2010. Complexities in barrier island response to sea level rise: Insights from numerical model experiments, North Carolina Outer Banks. *J. Geophys. Res.* doi:10.1029/2009JF001299
- Moore, L.J., McNamara, D.E., Murray, a. B., Brenner, O., 2013. Observed changes in hurricane-driven waves explain the dynamics of modern cusped shorelines. *Geophys. Res. Lett.* 40, 5867–5871. doi:10.1002/2013GL057311

- Murray, A.B., Gopalakrishnan, S., McNamara, D.E., Smith, M.D., 2013. Progress in coupling models of human and coastal landscape change. *Comput. Geosci.* 53, 30–38. doi:10.1016/j.cageo.2011.10.010
- NASA, 2010. Final programmatic environmental impact statement Wallops Flight Facility shoreline restoration and infrastructure protection program.
- National Park Service, 2002. Assateague Island National Seashore Long Range Interpretive Plan.
- Parris, A., Bromirski, P., Burkett, V., Cayan, D., Culver, M., Hall, J., Horton, R., Knuuti, K., Moss, R., Obeysekera, J., Sallenger, A., Weiss, J., 2012. Global Sea Level Rise Scenarios for the US National Climate Assessment. NOAA Tech Memo OAR CPO 1–37.
- Pfeffer, W.T., Harper, J.T., O’Neel, S., 2008. Kinematic constraints on glacier contributions to 21st-century sea-level rise. *Science* 321, 1340–1343. doi:10.1126/science.1159099
- Sallenger, A.H., Doran, K.S., Howd, P. a., 2012. Hotspot of accelerated sea-level rise on the Atlantic coast of North America. *Nat. Clim. Chang.* 2, 1–5. doi:10.1038/nclimate1597
- Schupp, C., 2013. Assateague Island National Seashore Geologic Resources Inventory Report.
- Slott, J.M., Murray, A. B., Ashton, A.D., 2010. Large-scale responses of complex-shaped coastlines to local shoreline stabilization and climate change. *J. Geophys. Res. F Earth Surf.* 115, F03033. doi:10.1029/2009JF001486
- Slott, J.M., Murray, A.B., Ashton, A.D., Crowley, T.J., 2006. Coastline responses to changing storm patterns. *Geophys. Res. Lett.* 33. doi:10.1029/2006GL027445
- Smith, M.D., Murray, A.B., Gopalakrishnan, S., Keeler, A.G., Landry, C.E., McNamara, D., Moore, L.J., 2015. , Chapter 7 – Geoengineering Coastlines? From Accidental to Intentional, in: *Coastal Zones, Solutions for the 21st Century*. Elsevier. doi:10.1016/B978-0-12-802748-6.00007-3
- Stive, M.J.F., de Vriend, H.J., 1995. Modelling shoreface profile evolution. *Mar. Geol.* 126, 235–248. doi:10.1016/0025-3227(95)00080-I
- Storlazzi, C.D., Shope, J.B., Erikson, L.H., Hegermiller, C.A., Barnard, P.L., 2015. Future Wave and Wind Projections for United States and United States-Affiliated Pacific Islands [WWW Document]. U.S. Geol. Surv. Open-File Rep. 2015–1001. doi:http://dx.doi.org/10.3133/ofr20151001
- U.S. Census Bureau, 2010. 2010 Profile of General Population and Housing Characteristics; Chincoteague town, Virginia. [WWW Document]. Online. URL http://factfinder.census.gov/faces/nav/jsf/pages/community_facts.xhtml (accessed 6.3.16).
- USFWS, 2015. Chincoteague and Wallops Island National Wildlife Refuges: Comprehensive Conservation Plan.
- Williams, S.J., 2013. Sea-level rise implications for coastal regions. *J. Coast. Res.* 63, 184–196. doi:10.2112/SI63-015.1
- Williams, Z.C., McNamara, D.E., Smith, M.D., Murray, a. B., Gopalakrishnan, S., 2013. Coupled economic-coastline modeling with suckers and free riders. *J. Geophys. Res. F*

Earth Surf. 118, 887–899. doi:10.1002/jgrf.20066

Woodruff, J.D., Irish, J.L., Camargo, S.J., 2013. Coastal flooding by tropical cyclones and sea-level rise. *Nature* 504, 44–52. doi:10.1038/nature12855

Zhang, K., Douglas, B.C., Leatherman, S.P., 2000. Twentieth-century storm activity along the U.S. East Coast. *J. Clim.* 13, 1748–1761. doi:10.1175/1520-0442(2000)013<1748:TCSAAT>2.0.CO;2